INVESTIGATION OF THE REACTIVITY OF THREE POLYHEDRAL BORANE ANIONS WITH ALBUMINS

THESIS

Presented to the Graduate Council of

Southwest Texas State University

In Partial Fulfillment of

The Requirements

For the Degree

Master of SCIENCE

By

William Jefferson McVey, B.S.

San Marcos, Texas

August 2003

ACKNOWLEDGEMENTS

There are a host of people who make possible the accomplishment of any endeavor by a single individual. This project, which has been seven years in the making, has been aided by many whose names I may forget, but whose importance to me is written in everything I do from this day forward. To the educators, some of whom have become dear friends, I say thank you for your devotion to your task.

I would like to thank the members of my committee, Dr. Linette M. Watkins and Dr. Lysle Kevin Lewis, both superb educators, and whom I count as friends. A very special thanks to Michelle Motley whose hard work on my behalf I will not forget. My lab mates still here, Jacqui, Skydiver Brian and those gone to other places, Sarah, Colby, and Andrew, have all played a part.

I would be horribly remiss if I did not single out two individuals whose presence, attentiveness, assertiveness, wisdom, care, and compassion have opened up my life to a universe of new possibilities. It has been either my blessing or my curse to have brilliant women in my life. My mother, Dollie, has been a fast friend in all waters and all weathers. She put a light in the window and wind in my sails so that I could find my way back home. Dr. Debra Feakes has believed in me, respected me, and taught me in spite of my stubborn resistance to being taught. The debt I owe is incalculable.

TABLE OF CONTENTS

LIST OF FIGURES

LIST OF TABLES

ABSTRACT

Boron neutron capture therapy (BNCT) has been proposed as a potential improvement on existing clinical modalities in the treatment of aggressive brain tumors, such as *gliobastoma multiforme*, and metastatic melanoma. Theoretically, BNCT is an ideal binary therapy in which each component is non-lethal. Boron-10 atoms, located in the tumor, react with thermal neutrons to produce an alpha particle and a lithium-7 particle. The energy produced by the reaction dissipates in a distance of approximately 8-10 μm in tissue.[1] The application of BNCT is dependant on the site specific delivery, and retention, of high concentrations of boron-containing compounds to the tumor.

Unilamellar liposomes have permitted the selective delivery of water soluble, polyhedral borane anions that have no inherent tumor specificity.[2-4] Murine biodistribution studies have established the retention of certain polyhedral borane anions within the tumor; however, the chemical nature of the retention has not been ascertained.[2-4] Researchers have proposed that certain polyhedral borane anions will react with nucleophilic sites on proteins or, in the case of a boron-containing compound which possesses a thiol substituent, form a disulfide bond. Although this hypothesis has been used for the design of new compounds, there has been no research to date to support the hypothesized formation of a covalent bond by any of the proposed mechanisms.[4]

Three polyhedral borane anions were selected for evaluation based on their *in vivo* murine biodistributions. The compounds were allowed to react with serum albumins and the products of the reaction were evaluated by gel electrophoresis, matrix assisted laser desorption mass spectroscopy (MALDI-MS), UV-Vis spectroscopy, and HPLC.

Additionally, a well established protocol using DTNB provided a significant indication of disulfide bond formation between a polyhedral borane anion possessing a thiol substituent and bovine serum albumin.[5] The results indicate that complexes are formed between the albumins and at least two of the polyhedral borane anions. The protein boron complexes are highly resistant to disruption, leading to the conclusion that a covalent bond, while not certain, is a possibility. Further testing of the existing complexes will be necessary to confirm the formation of a covalent bond and to locate the binding sites.

CHAPTER 1

INTRODUCTION

Current therapeutic protocols that treat highly aggressive forms of brain cancer, such as *gliobastoma multiforme* and metastatic melanoma, rely initially on surgical extirpation of the malignancy. As a result, there is an inherent uncertainty as to whether residual cells are left behind to become the foci of new tumor growth in the original or other locations. Although most tumors of the brain appear to exhibit little propensity to metastasize to other organs, they do possess a tendency to infiltrate the brain itself.[1] Any effective cancer therapy would have to destroy or inhibit the growth of these residual cells without compromising the normal cells from which they are derived in order to improve a patient's probability of survival and quality of life. The existing treatment modality to deal with the residual cells and the infiltration has been the synergistic combination of conventional radiotherapy and cytoreductive chemotherapy.[1]

The dose associated with conventional radiotherapy results in the damage of nearby normal brain cells. Likewise, the chemotherapeutic agents have to be limited to the tolerance of normal cells and thus are not completely effective at killing the remaining cancer cells. Consequently, these two modalities have been used synergistically in fractionated doses in the hope of moderating the toxic effects to normal brain tissue. One problem with this strategy arises because of the resistance of highly malignant brain tumors to conventional radiotherapy and chemotherapy. The second problem associated with the fractionated doses is the reduction in the quality of life as a result of the treatment. The selective destruction of brain tumor cells remains an

unachieved goal in current treatment modalities. Consequently, boron neutron capture therapy (BNCT) has been proposed as a potential improvement on existing clinical modalities.

Boron is a metalloid that has an average atomic mass of 10.81 amu based on the two naturally occurring isotopes, boron-11 and boron-10. The two isotopes of boron are similar in structure and chemical reactivity. The unique characteristic that suggests the possibility for a cancer therapy lies in the extremely high neutron capture cross section of the boron-10 isotope, with a neutron capture cross section of 3838 barns. While there are a number of elements with large neutron capture cross sections, boron is one of the easiest to manipulate chemically, is a stable isotope, and is present in relatively high abundance (Table 1).[2] In addition, the thermal neutron-capture cross-section of

Nuclide	Cross-Section (Barns)	Natural Abundance (%)
^{6}Li	942	7.5
^{10}B	**3838**	**19.8**
^{113}Cd	19800	12.2
^{149}Sm	42000	13.9
^{155}Gd	61000	14.8
^{157}Gd	255000	15.7
^{235}U	580	0.72

Table 1: Elements with large neutron capture cross-sections and their natural abundances

physiologically abundant atoms (Table 2) is extremely low in comparison.[2] Therefore, the large neutron capture cross-section of boron-10, relative to the elements in human tissue, enables the selective neutron capture of boron present in tumor cells.

Nuclide	Cross-Section (Barns)	Natural Abundance (%)
^{1}H	0.332	99.8
^{12}C	0.0034	98.9
^{14}N	1.82	99.6
^{16}O	0.00018	99.8
^{23}Na	0.43	100.0
^{31}P	0.18	100.0
^{32}S	0.53	95.0
^{35}Cl	32.68	76.0

Table 2: Neutron capture cross-sections of physiologically abundant elements

Once the boron-10 nuclei capture a thermal neutron, an unstable boron-11 isotope is formed which undergoes a fission reaction. The fission reaction produces an energetic helium-4 (alpha) particle and a recoiling lithium-7 ion (Figure 1).[3] The range of these particles in tissue is approximately 8-10 μm which corresponds to about one cell diameter. The combined average kinetic energy of the particles is 2.31 MeV. Tumor cells selectively loaded with sufficiently high concentrations of boron-10 can, theoretically, be destroyed once the neutron capture reaction takes place.[4]

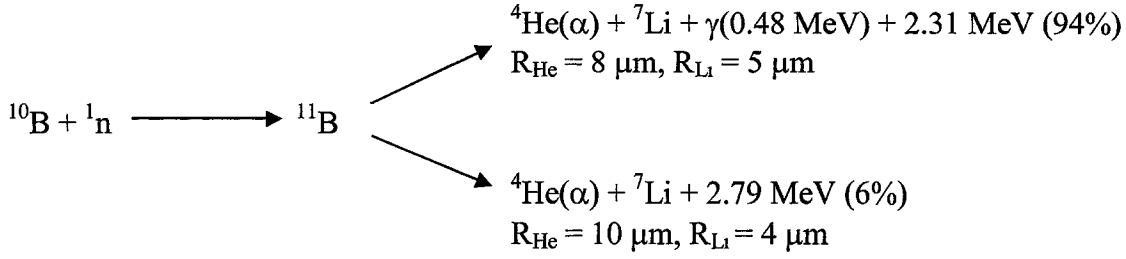

Figure 1: Neutron capture reaction

Currently, the major limitation of the therapy is that large concentrations of boron are required in each tumor cell. In order for BNCT to constitute a successful therapy, the estimated theoretical concentration required is calculated to be approximately 15 μg of boron per gram of tissue.[5] The accuracy of these calculations is dependent on the location of the boron target nuclei within the tumor cell. Since the genetic material in the nucleus of the tumor cell is the ultimate target of the lethal particles, the proximity of the boron to that location is critical to the amount required for tumor destruction. Consequently, the concentration of the boron target nuclei can be much less if the boron is localized near the nuclear material of the tumor cell rather than on the exterior cell wall. The surrounding normal tissue, including blood, must have a minimal concentration of boron target nuclei to reduce the lethal effects on normal tissue.

Theoretically, BNCT is an ideal binary therapy in which each component is non-lethal. As attractive as BNCT might appear to be, significant limitations have been encountered in past applications of BNCT. BNCT trials were performed in the 1950s and 1960s by both Brookhaven National Laboratories (BNL) and the Massachusetts Institute of Technology (MIT). In those trials, $Na_2[B_4O_7]$ and $Na_2[B_{10}H_{10}]$ were injected into malignant gliomas and the tumors were irradiated with thermal neutrons.[1] The results, which were not spectacular, were attributed to the poor tumor specificity of the compound, and insufficient penetration of the thermal neutrons.[3] Although the penetration issue was solved by a partial resection of the scalp and skull as well as the use of an isothermal neutron beam, the poor tumor specificity associated with the compounds is still an issue with the application of BNCT.

Since the original clinical trials in the 1950's and 1960's, some encouraging results have been obtained using BNCT for the treatment of malignant brain tumors and metastatic melanoma. The Hatanaka group in Japan used boron-10 enriched borocaptate sodium ($Na_2B_{12}H_{11}SH$, BSH) (Figure 2) and clinical trials in the United States have been using *p*-boronophenylalanine (*p*-BPA) (Figure 3).[1] The two compounds have been shown to accumulate in the tumor of a number of small animal glioma models.[6-8] Retention of BSH has been attributed to the formation of disulfide bonds within the tumor cell while the retention of BPA has been attributed to incorporation of the compound into a metabolic cycle.[1]

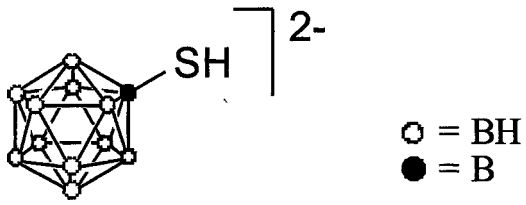

Figure 2: Structure of $Na_2[B_{12}H_{11}SH]$ (BSH)

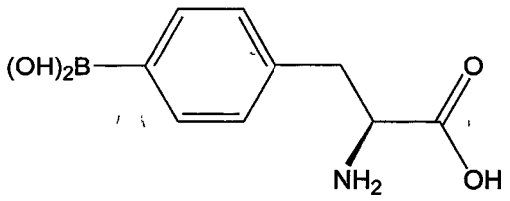

Figure 3: Structure of *p*-BPA

Even though BSH and *p*-BPA are currently being used for BNCT, the compounds lack the desired retention properties and localization within the tumor to be truly viable

cancer agents. Therefore, the design and preparation of boron-containing compounds for application in BNCT is currently the basis for extensive research. At present, two general methods have been utilized in the development of compounds for evaluation as BNCT agents. One method is based on the synthesis of boron-containing derivatives of species known to accumulate in the tumor or that have the potential for *in vivo* metabolization. This category includes boron derivatives of amino acids,[9-11] nucleosides and nucleotides,[12-15] monoclonal antibodies,[16] and porphyrins.[17,18] The second method is based on the design of a delivery system that deposits a boron-containing compound that has no inherent tumor specificity. While low-density lipoproteins incorporating lipophilic boron-containing compounds have been studied,[19] the primary system used in this category is the utilization of unilamellar liposomes as delivery vehicles.[20-23]

For a number of years, liposomes have been studied as medicinal delivery agents. Liposomes have been employed as tumor selective delivery vehicles for radiopharmaceuticals used in both animal models and in human diagnosis.[24-26] Synthetic liposomes are free of receptor-seeking functionalities and are selectively internalized by tumor masses. For small, unilamellar liposomes, the immature and consequently abnormally porous vasculature of a rapidly growing tumor mass is thought to be responsible for the cellular differentiation process. The process of internalization is proposed to arise by nonspecific endocytosis of the coated pit-coated vesicle type.[27] In the case of a coated vesicle, the vesicle ruptures and the contents are released into the cytoplasm of the cell.[27] The retention of the compounds released by the liposome varies, possibly according to their size, charge, and the ability of the compound to interact with the intracellular protein moieties.

Liposomes are appealing for application as delivery agents in BNCT because a wide variety of boron-containing compounds can be incorporated into the liposome structure. The aqueous interior of the liposomes can carry hydrophilic boron-containing compounds and the lipophilic bilayer is capable of carrying hydrophobic boron-containing compounds. While both hydrophilic and hydrophobic boron-containing compounds have been prepared for incorporation into the liposomes, the majority of the previous research, and the emphasis of the current research, are water soluble polyhedral borane anions which are encapsulated in the aqueous interior of the liposomes.

The liposomes that have been studied for application in BNCT, and used in recent investigations, are of a specific size and composition (Figure 4). Unilamellar liposomes ranging from 50-90 nm in diameter are used for the BNCT investigations. The small size

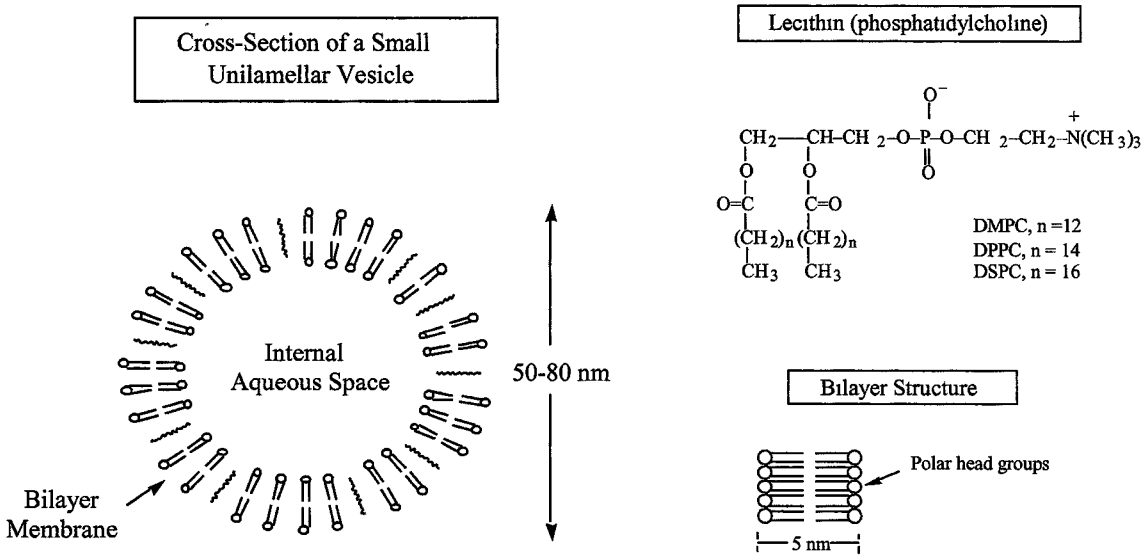

Figure 4: Unilamellar liposomes and bilayer constituents

of the liposomes is ideal for passing through the holes in the immature vasculature characteristic of rapidly growing tumor masses, thereby selectively depositing the liposomes and their contents into the tumor mass. The bilayer is composed of an equimolar mixture of cholesterol and 1,2-distearoyl-sn-glycero-3-phosphocholine (DSPC). The addition of cholesterol to the bilayer and the use of pure, synthetic phospholipids, as opposed to natural phospholipids, enhances the bilayer stability. The concentration of boron required for the application of BNCT is obtained by the encapsulation of hypertonic solutions of the polyhedral borane anions ranging from 750-900 mOsM. Higher concentrations of the water-soluble polyhedral borane anions cannot be encapsulated due to the detrimental effects to the stability of the liposome formulation.

Once the boron-containing liposomes were prepared, biodistribution studies were conducted in the laboratories of Dr. Patrick R. Gavin at Washington State University (Pullman, WA) by implanting BALB/c mice with EMT6 mammary adenocarcinomas in the right or left flank. The liposome formulation was injected in the tail vein. The mice were sacrificed at each time increment, typically 5-6 time points, in a 48-hour time period. The results are depicted with boron concentration plotted on the y-axis and time plotted on the x-axis. The boron concentration in selected tissues were measured by inductively coupled plasma-atomic emission spectroscopy (ICP-AES) in the laboratories of Dr. William Bauer at the Idaho National Engineering and Environmental Laboratories (INEEL). A minimal biodistribution experiment would include tumor, blood, liver, and spleen analysis.

Many water-soluble, polyhedral borane anions have been incorporated into unilamellar liposomes and investigated in murine biodistribution studies. While several

of these polyhedral borane anions have rapidly cleared from all tissues in the biodistribution experiments, others have demonstrated a high degree of tumor uptake, and retention, at low injected doses relative to other methods investigated for application in BNCT.[28-33] Researchers have hypothesized that compounds which have the potential to react with intracellular protein moieties will be retained by the tumor while compounds which lack this reactivity will be rapidly cleared from all tissues, including tumor.

The polyhedral borane anion, $[B_{10}H_{10}]^{2-}$ (Figure 5), was the first boron-containing compound investigated in murine biodistribution experiments.[20] The dianion is

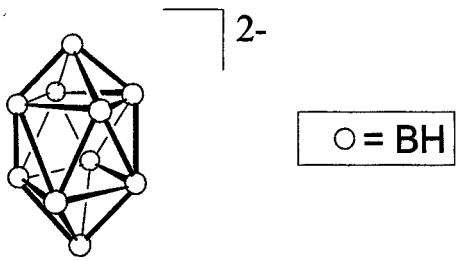

Figure 5: Structure of $[B_{10}H_{10}]^{2-}$

characterized by two equivalent apical B-H vertices and eight equivalent equatorial B-H vertices. The negative two charge is delocalized over the entire cage. Under physiological conditions, The $[B_{10}H_{10}]^{2-}$ is unreactive. Encapsulation of the $[B_{10}H_{10}]^{2-}$ anion in unilamellar liposomes, followed by evaluation in an *in vivo* murine biodistribution experiment, demonstrated that this anion is cleared rapidly from all tissues, including blood.[20] Oxidative coupling of two $[B_{10}H_{10}]^{2-}$ ions yields the $[B_{20}H_{18}]^{2-}$ anion.

The $[B_{20}H_{18}]^{2-}$ anion is composed of two $[B_{10}H_9]^-$ cage fragments linked by a pair of three-center, two-electron bonds between two boron atoms. Incorporation of the $[B_{20}H_{18}]^{2-}$ anion into unilamellar liposomes and evaluation in the biodistribution experiments was appealing for two reasons. First, the amount of boron is doubled per unit charge, relative to $[B_{10}H_{10}]^{2-}$, thereby increasing the concentration of boron without increasing the osmotic stress on the liposome bilayer. Second, due to the presence of the electron-deficient bonding region, the $[B_{20}H_{18}]^{2-}$ anion is susceptible to nucleophilic attack. Simple nucleophiles, such as hydroxide, alkoxide, and amide, react with the electron-deficient bonding region to produce the reduced, substituted anions of the form $[B_{20}H_{17}X]^{4-}$ where X is the nucleophilic group.[3,21,34,35] The reaction with hydroxide is depicted in Figure 6. Also shown is the photoisomerization of $[n\text{-}B_{20}H_{18}]^{2-}$ to an isomer designated as $[i\text{-}B_{20}H_{18}]^{2-}$ which is subject to nucleophilic attack as well. The $[B_{20}H_{18}]^{2-}$ ion can be reversibly reduced to form the unsubstituted $[B_{20}H_{18}]^{4-}$ anion.

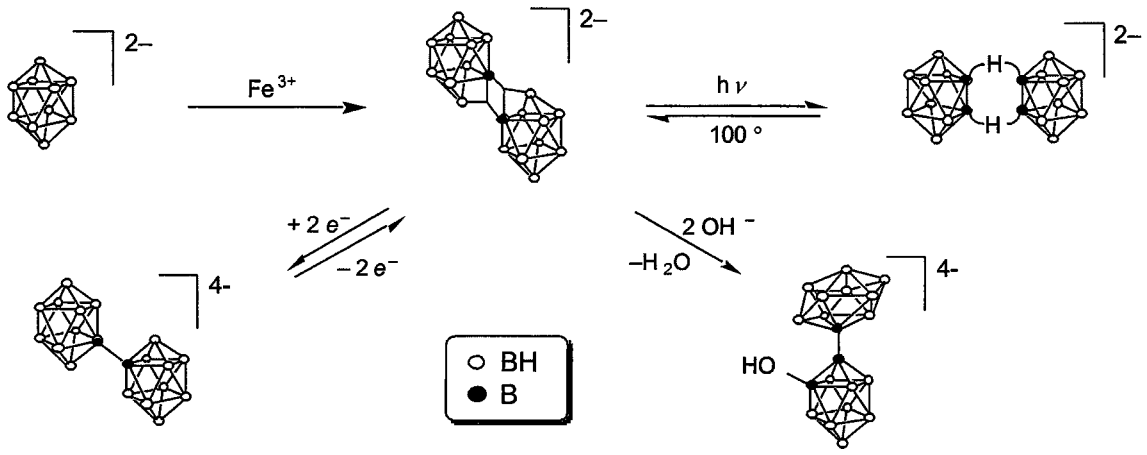

Figure 6: Reactions of $[B_{20}H_{18}]^{2-}$

All of the compounds depicted in Figure 6 have been encapsulated in unilamellar liposomes and investigated in murine biodistribution experiments.[20] The unreactive anions, $[B_{10}H_{10}]^{2-}$, $[B_{20}H_{17}OH]^{4-}$ and $[B_{20}H_{18}]^{4-}$ are rapidly cleared from all tissues, while the reactive compounds, $[n\text{-}B_{20}H_{18}]^{2-}$ and $[i\text{-}B_{20}H_{18}]^{2-}$ are retained by the tumor.[20] These results supported the hypothesis that compounds capable of reaction with intracellular protein moieties are retained by the tumor. In an attempt to understand the mechanisms of retention, the ammonio derivative, $[B_{20}H_{17}NH_3]^{3-}$, was prepared, encapsulated in unilamellar liposomes, and evaluated in a murine biodistribution experiment (Figure 7).[21]

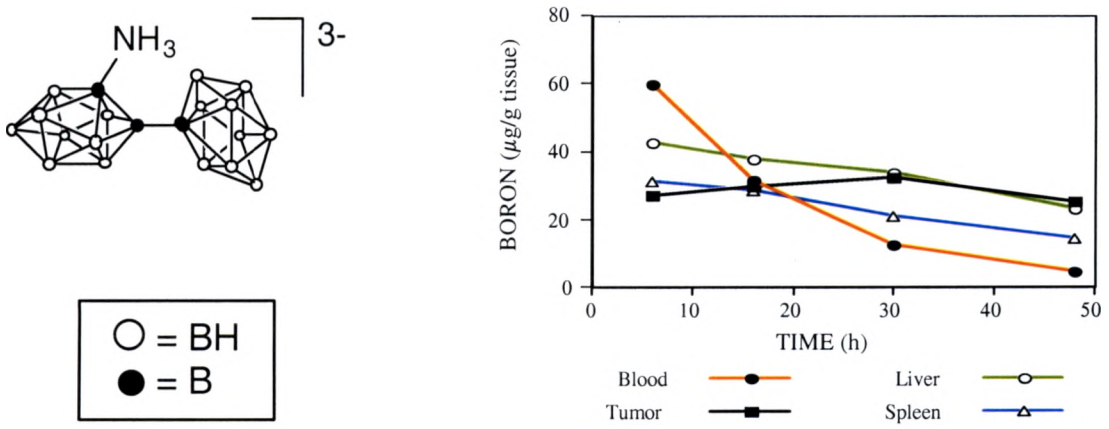

Figure 7: Structure of the ammonio anion, $[B_{20}H_{17}NH_3]^{3-}$, and the *in vivo* murine biodistribution

The ammonio anion was the first to show an increase in tumor boron concentration in the time course experiment. The accretion of the ammonio compound was unexpected and led researchers to hypothesize a possible mechanism by which a covalent bond could be formed between a polyhedral borane anion and an intracellular protein moiety.[21] In the proposed mechanism, the ammonio compound is oxidized *in vivo* to form the more reactive $[B_{20}H_{17}NH_3]^-$ ion. The $[B_{20}H_{17}NH_3]^-$ ion, analogous to the

$[B_{20}H_{18}]^{2-}$ anion, is susceptible to nucleophilic attack at the electron-deficient, three center, two electron bonding region. The negative one charge should make the ion even more susceptible to nucleophilic attack than the $[B_{20}H_{18}]^{2-}$ ion.

Based on the proposed mechanisms of retention for the $[B_{12}H_{11}SH]^{2-}$ anion and the $[B_{20}H_{17}NH_3]^{3-}$ anion, the synthesis and evaluation of $[a^2\text{-}B_{20}H_{17}SH]^{4-}$ anion was proposed. The $[a^2\text{-}B_{20}H_{17}SH]^{4-}$ anion could potentially form disulfide bonds with cysteine residues (Figure 8), similar to that proposed for BSH, or it could oxidize to the more reactive $[B_{20}H_{17}SH]^{2-}$ anion, susceptible to nucleophilic attack (Figure 8), similar to that proposed for the $[B_{20}H_{17}NH_3]^{3-}$ anion.

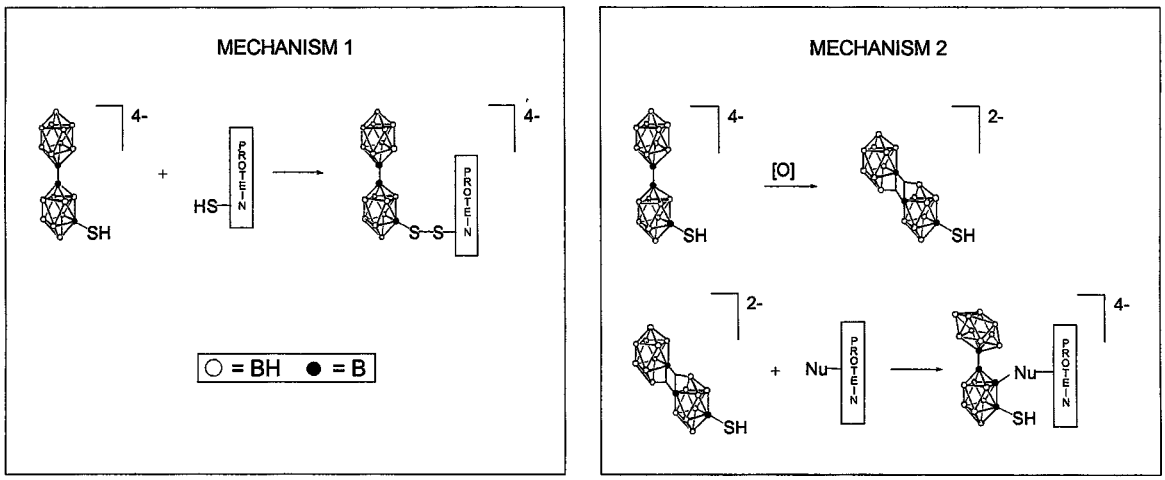

Figure 8: Proposed mechanisms of retention of the $[B_{20}H_{17}SH]^{4-}$ anion

Based on these potential mechanisms of retention, the $[B_{20}H_{17}SH]^{4-}$ anion was synthesized in the laboratories of Dr. Debra A. Feakes at Southwest Texas State University and submitted for murine biodistribution analysis. The results of the analysis (Figure 9) demonstrate that the unique feature of the $[a^2\text{-}B_{20}H_{17}SH]^{4-}$ anion is that the

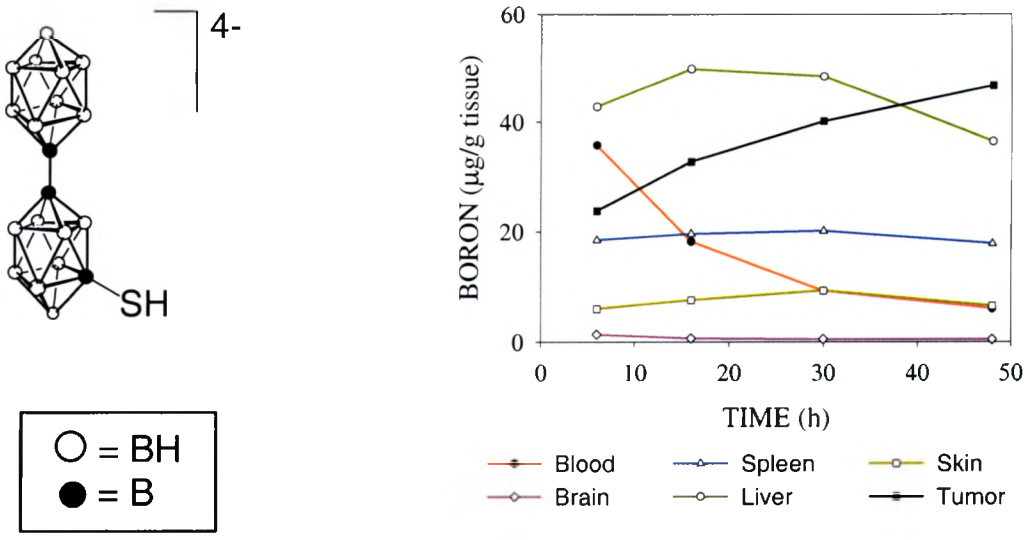

Figure 9: Murine biodistribution of $Na_4[B_{20}H_{17}SH]$ encapsulated in unilamellar liposomes

boron concentration accretes in the tumor over the 48 hour test period while simultaneously washing out of the blood.[23] To date, the $[B_{20}H_{17}SH]^{4-}$ anion is the only polyhedral borane anion which exhibits this behavior. The unusual result supports the possible formation of a disulfide bond between the sulfhydryl on the anion and a free cysteine on an intracellular protein, oxidation of the anion to the more reactive species, and/or both mechanisms working in the same environment.

CHAPTER 2

STATEMENT OF PROBLEM

For many years, researchers have proposed that the fate of a polyhedral borane anion, encapsulated in unilamellar liposomes and delivered to the tumor *in vivo*, is dependent on the reactivity of the anion. Biodistribution results have demonstrated that electrophilic compounds are better suited for long-term retention within a tumor cell due to the susceptibility to attack by nucleophiles. The studies have demonstrated that some compounds are retained by the tumor over a period of time while others are cleared from the tumor. Researchers have proposed that compounds that have the potential to react with intracellular protein moieties are retained by the tumor, and compounds that do not have the potential to react with intracellular protein moieties are cleared from the tumor. Although many amino acids, such as cysteine or tyrosine, as well as metabolites that proliferate in the cell, should possess sufficient nucleophilicity to react with the electrophilic boron-containing anions, no investigations have been reported which demonstrate that the polyhedral borane anions covalently bind to proteins.

The goal of the research project is to ascertain whether covalent binding exists between select polyhedral borane anions and either bovine serum albumin or human serum albumin. The three polyhedral borane anions selected for investigation are the $[B_{20}H_{17}SH]^{4-}$, $[B_{20}H_{18}]^{2-}$, and $[B_{20}H_{17}OH]^{4-}$ anions. These ions were selected based on the ability of the anions to be retained in the tumor in *in vivo* murine biodistribution experiments. The ions were synthesized, allowed to react with bovine serum albumin and human serum albumin, and the products of the reactions were evaluated by a variety

of analytical techniques including SDS-PAGE, MALDI-MS, HPLC, and CZE. An understanding of the potential mechanisms of retention and the potential binding sites for this class of compounds should provide a method to predict, *a priori*, compounds that would exhibit enhanced retention and, thereby, focus the synthetic research on compounds with a high probability for success.

CHAPTER 3

MATERIALS AND METHODS

Synthesis

Materials. Synthetic reactions were performed under an argon atmosphere using Schlenk techniques where necessary. The polyhedral borane starting materials were prepared by published methods.[23,35-37] The Bender's salt, $K[SC(O)OC(CH_3)_3]$, was prepared using the methods reported by Daly and Lee.[38] Tetrahydrofuran (THF) was distilled from sodium metal prior to use. Distearoylphosphatidylcholine (DSPC) was obtained from Avanti Polar Lipids and the cholesterol was supplied by Sigma Chemical Company. Decaborane was obtained from KatChem (Czechoslovakia) and used as received. **CAUTION:** ***Decaborane is a highly toxic, impact sensitive compound which forms explosive mixtures, especially with halogenated materials. A careful examination of the MSDS is recommended before usage.*** All other reagents were purchased from Aldrich Chemical Company and used without further purification.

Physical Measurements. The ^{1}H, ^{13}C, and ^{11}B NMR Fourier transform NMR spectra were obtained with a Varian INOVA instrument operating at 400 MHz, 100 MHz, and 128 MHz, respectively. Proton and carbon chemical shifts were referenced to residual solvent protons. Boron chemical shifts were externally referenced to $BF_3 \bullet Et_2O$ in $C_6{}^2H_6$; peaks upfield of the reference are designated as negative. The Fourier transform IR spectra were obtained as nujol mulls using a Perkin-Elmer 1300 instrument. The spectroscopic details for each of the compounds are not reproduced. All spectra correlated with the known and reported spectra of the compounds.

$(Et_3NH)_2B_{10}H_{10}$. Decaborane ($B_{10}H_{14}$, 30.5 g, 0.250 mol) was placed in a 1 L three-necked flask equipped with a pressure equalizing dropping funnel (PED), mechanical stirrer, and a condensing column. The decaborane was dissolved in 300 mL of xylene under a positive pressure of argon. An excess of triethylamine, Et_3N, was added dropwise at room temperature to the solution over a five minute period utilizing the PED. The flask was placed on a heating mantle, heated to approximately 100 °C, and the mixture stirred for approximately three hours during which the first evolution of hydrogen gas occurred. After three hours, the reaction mixture was allowed to reflux for three hours and then allowed to cool to room temperature. The contents were transferred to a 600 mL sintered glass frit. The precipitate was separated from the xylene by vacuum filtration and washed twice in the same frit with 50 mL of isopropanol and once with 100 mL anhydrous diethyl ether. The solid was dried under vacuum in a 500 mL round bottom flask for 24-hours. The crude white product was transferred to a 600 mL beaker and dissolved in approximately 100 mL of boiling distilled water (DI). The solution was filtered in a large, hot frit and the filtrate collected in a 1 L Erlenmeyer filter flask. The filter flask was put on the hot plate, the solution brought to boiling, and absolute alcohol (~800 mL) was added until a white precipitate persistently formed. The solution was allowed to boil until it was again clear. The filter flask was allowed to cool until a milky white precipitate formed. The precipitate was filtered and washed with 500 mL of isopropanol and 100 mL of anhydrous diethyl ether. The product was transferred to a 500 mL round bottom flask and dried under vacuum. The white crystalline product was isolated in 74.2 % yield.

$Na_2[B_{10}H_{10}]$. Solid $(Et_3NH)_2B_{10}H_{10}$ (20.0 g, 0.0620 mol) was transferred to a 250 mL beaker and dissolved in 125 mL of distilled water to produce an approximately 0.5 M solution. A 2.0 molar excess of NaOH was added to the solution and the solution was allowed to stir for thirty minutes. The solution was poured into a 250 mL separatory funnel and washed three times with 50 mL aliquots of hexane to remove the triethylamine. The hexane layer was discarded following each washing and the aqueous layer was saved. The transparent, pale yellow solution contained the sodium salt of $[B_{10}H_{10}]^{2-}$.

$Na_2[B_{20}H_{18}]$. The $Na_2[B_{10}H_{10}]$ solution was acidified with 12 M HCl and placed in a three-necked round bottom flask (1 L) fitted with a condensing column, PED, and a stir bar. An excess of $FeCl_3 \bullet 6H_2O$ (50.0 g, 0.185 mol) was dissolved in approximately 150 mL of DI water and added to the dropping funnel. The three-necked round-bottomed flask was placed on a heating mantle on top of a magnetic stirrer and allowed to reflux. The $FeCl_3 \bullet 6H_2O$ was added dropwise over 15 minutes. The solution was refluxed for five hours. The resulting solution was a yellow green color. The reaction was allowed to cool to room temperature in the round bottom flask.

$Cs_2[B_{20}H_{18}]$. A solution of cesium chloride, CsCl, in DI water was prepared by mixing 13 g CsCl (0.077 mol) and 50 mL DI water. The CsCl solution was added to the yellow-green solution containing $Na_2[B_{20}H_{18}]$. A pale yellow precipitate began to form immediately. The flask containing the precipitate and the solution was cooled to 4 °C in an ice bath. The mixture was filtered through a sintered glass frit to isolate the solid. The solid was dried for 24 hours and recrystalized from a minimum amount of boiling water.

The yellow crystalline product was isolated by filtration of the mixture and allowed to dry overnight. The product was isolated in 83 % yield.

$Na_2[B_{20}H_{18}]$. An ion exchange column was prepared by packing a slurry of ion exchange resin (Dowex 50 X 8-100) and distilled water into an 800 mL column. The column resin was washed with distilled H_2O until the eluent was clear (approximately 2 L). Approximately one liter of 1 M NaOH was eluted through the column to convert the column to the Na^+ form. The resin becomes a darker color during the process. Distilled water was eluted through the column to remove excess base. The process was monitored using pH paper. The resin in the column was converted to the acid form by eluting approximately one liter of 1 M HCl through. Excess acid was removed by a second elution of distilled water through the column until the pH of the eluent was neutral. The resin was equilibrated with 2.5:1 DI H_2O:CH_3CN mixture. $Cs_2[B_{20}H_{18}]$ was dissolved in a minimum amount of acetonitrile and distilled H_2O was added to the solution until a 2.5:1 H_2O:CH_3CN mixture was achieved. The column was loaded with the $Cs_2[B_{20}H_{18}]$ solution. Additional H_2O:CH_3CN was added to the top of the column, and the eluent was monitored by pH paper. The neutral solution was collected until an acidic pH was observed. At that point, a separate collection vessel was used to collect the solution until a neutral pH was observed. Rotary evaporation was used to remove the acetonitrile. The aqueous solution was titrated with standardized NaOH (0.9603 M). The remaining water was removed under vacuum and ^{11}B NMR was performed on the solid to confirm the product identity. The solid was dissolved in a minimum amount of DI H_2O and the solution transferred to a 25 mL volumetric flask. Water washes of the flask were added

to bring the volume to the mark. The resulting solution (361 mM) was filtered through a 0.22 μm filter and stored for further use.

$K_4[B_{20}H_{17}OH]$. An aqueous solution of $Na_2[B_{20}H_{18}]$ (25 mL, 0.361 M) was transferred to a 100 mL beaker. Two molar equivalents of NaOH were dissolved in a minimum amount of distilled water. The solution of $Na_2[B_{20}H_{18}]$ was equipped with a small magnetic stir bar and placed on a stir plate. The NaOH solution was added to the $Na_2[B_{20}H_{18}]$ solution and allowed to stir for two hours at room temperature. A saturated solution of potassium acetate, $KC_2H_3O_2$, in absolute ethanol was prepared and added to the $Na_4[B_{20}H_{17}OH]$ solution until the resulting white precipitate ceased to form. The white precipitate was isolated by filtration through a small frit and allowed to air dry over the weekend. The crude product was dissolved in 45 mL of 1 M HCl and allowed to stir at room temperature for one hour. An excess of KOH was added dropwise while stirring with a magnetic stirrer until the pH was greater than 9. The solution was filtered by gravity filtration to remove particulate matter. Absolute ethanol was added to a warmed, stirred, solution of the product until the precipitate failed to dissolve for a minute or more. The solution was cooled to room temperature, covered with parafilm, and stored in the refrigerator. The precipitate was filtered in a sintered glass frit and washed with ethanol. The precipitate was transferred to a Schlenk flask and dried under vacuum. A second crop of product was harvested from the filtrate using the same technique. The two crops were combined and dissolved in a minimum amount of water.

$Na_4[B_{20}H_{17}OH]$. An ion exchange column was prepared by packing a slurry of ion exchange resin (Dowex 50 X 8-100) and distilled water into an 800 mL column. The column resin was washed with distilled H_2O until the eluent was clear (approximately 2

L). Approximately one liter of 1 M NaOH was eluted through the column to convert the column to the Na^+ form. The resin becomes a darker color during the process. Distilled water was eluted through the column to remove excess base. The process was monitored using pH paper. The resin in the column was converted to the acid form by eluting approximately one liter of 1 M HCl through. Excess acid was removed by a second elution of distilled water through the column until the pH of the eluent was neutral. The resin was equilibrated with DI H_2O. $K_4[B_{20}H_{17}OH]$ was dissolved in a minimum amount of distilled H_2O. The column was loaded with the $K_4[B_{20}H_{17}OH]$ solution. Additional H_2O was added to the top of the column, and the eluent was monitored by pH paper. The neutral solution was collected until an acidic pH was observed. At that point, a separate collection vessel was used to collect the solution until a neutral pH was observed. The aqueous solution was titrated with standardized NaOH (0.9603 M). The remaining water was removed under vacuum and ^{11}B NMR was performed on the solid to confirm the product identity. The solid was dissolved in a minimum amount of DI H_2O and the solution transferred to a 25 mL volumetric flask. Water washes of the flask were added to bring the volume to the mark. The resulting solution (272 mM) was filtered through a 0.22 μm filter and stored for further use.

$K[SC(O)OC(CH_3)_3]$. A hot 1 L three-necked round bottom flask was equipped with a condenser, adapter with stopcock, and septa, and cooled under argon. Freshly distilled tetrahydrofuran (THF, 50 mL) was transferred to the flask using Schlenk techniques. THF, dimethylformamide (150 mL) and a solution of potassium t-butoxide in t-butanol (1 M, 520 mL) were transferred to the reaction flask. The reaction flask was cooled in an ice and NaCl bath and the mixture stirred for 15 minutes. A carbonyl sulfide

gas tank was placed on a balance and supported with a clamp. A piece of tygon tubing equipped with a 12 inch 18 gauge needle was inserted into the reaction flask through the septa on one end and the balance was zeroed. The gas was bubbled through the solution until the scale read -42.0 g. As soon as the gas flowed into the reaction mixture, a white precipitate began to form. The final solution was brown in color. The solution was raised to room temperature and stirred for 12 hours. The slurry was filtered through a frit under an argon atmosphere and the off-white solid dried under vacuum. The identity of the product was confirmed by ^{1}H NMR and IR spectroscopy.

$K_4[B_{20}H_{17}SC(O)OC(CH_3)_3]$. $(Et_3NH)_2B_{20}H_{18}$ (6.0 g, 0.019 mol) and Benders Salt (14.8 g, 0.0860 mol) were placed in a Schlenk flask with 300 mL of freshly distilled THF. The mixture was stirred in a closed flask under positive pressure of argon for six days. Each working day the reaction mixture was allowed to settle. A sample of the top layer was extracted while under argon and an IR performed to detect the presence of boron. Boron remaining in the solution indicated an incomplete reaction. When the reaction was complete, the reaction mixture was filtered and washed with THF. The solid was washed with anhydrous diethyl ether and then dissolved in 50 mL of DI water and filtered by gravity filtration. Ethanol was added to the warm (50 °C) mixture until cloudy. The mixture was cooled overnight and a precipitate formed. The solid was isolated using a sintered glass frit. The second crop was recrystalized from the original filtrate. The third crop was acquired by dissolving the precipitate on the inside of the filter flask in water and recrystallizing. All three crops were combined and dried under vacuum to give the product in 75 % yield.

$K_4[B_{20}H_{17}SH]$. Hydrochloric acid (HCl, 50 mL, 1 M) was added to the protected thiol compound, $K_4[B_{20}H_{17}SC(O)OC(CH_3)_3]$. Gas evolution was evident. The solution was stirred for 2 hours at room temperature. A concentrated solution of KOH was added to the mixture to remove the bridge proton. The mixture was warmed to 70 °C and ethanol was added to precipitate the product. The solution was cooled overnight. The crystals were filtered in a frit and washed with ether. The product was put under vacuum in a Schlenk flask. The IR and NMR (carbon and proton) spectra indicated small amounts of an impurity in the $K_4[B_{20}H_{17}SH]$. The impurity is believed to be $K_4[B_{20}H_{17}OCH_2CH_2CH_2CH_3]$, formed as a result of ring opening of the THF solvent and subsequent reaction with the $[B_{20}H_{18}]^{2-}$ anion.

$Na_4[B_{20}H_{17}SH]$. An ion exchange column was prepared by packing a slurry of ion exchange resin (Dowex 50 X 8-100) and distilled water into an 800 mL column. The column resin was washed with distilled H_2O until the eluent was clear (approximately 2 L). Approximately one liter of 1 M NaOH was eluted through the column to convert the column to the Na^+ form. The resin becomes a darker color during the process. Distilled water was eluted through the column to remove excess base. The process was monitored using pH paper. The resin was equilibrated with DI H_2O. $K_4[B_{20}H_{17}SH]$ was dissolved in a minimum amount of distilled H_2O. The column was loaded with the $K_4[B_{20}H_{17}SH]$ solution. Additional H_2O was added to the top of the column, and the eluent was monitored using silver nitrate. The solution was collected until a positive silver nitrate test was observed. At that point, a separate collection vessel was used to collect the solution until a positive silver nitrate test was not observed. The water was removed under vacuum and ^{11}B NMR was performed on the solid to confirm the product identity.

The solid was dissolved in a minimum amount of DI H_2O and the solution transferred to a 25 mL volumetric flask. Water washes of the flask were added to bring the volume to the mark. The resulting solution (260 mM) was filtered through a 0.22 μm filter and stored for further use.

Reaction of Polyhedral Borane Anions and Albumins. A stock solution of the protein, either BSA or HSA, was prepared by dissolving 100.2 mgs in 10 mL of phosphate buffered saline (0.10 M, pH 7.36). Four aliquots of the stock solution, 2.5 mL each, were transferred to four reaction tubes. An aqueous solution of each of the three polyhedral borane compounds, in the appropriate amount to provide a 100-fold excess, was added to each of three reaction tubes. The fourth reaction tube did not receive any polyhedral borane anion and served as a control. The reaction tubes were sealed and immersed in a water bath at 37 °C. After 36 hours, the reaction tubes were removed from the water bath and the reaction mixtures were filtered using millipore centricon filters with a pore size of 30,000 Daltons to remove the buffer and the excess polyhedral borane compound. The residue that was filtered from the reaction mixture was washed with ultra pure water, vortexed, and filtered again until a total volume of 10 mL of water had been used in the washing. The washed residue was reconstituted in 0.10 M PBS at a pH of approximately 8. The residue was analyzed by ^{11}B NMR spectroscopy to ascertain whether there was any detectable amount of unreacted polyhedral borane compound remaining in the mixture. If a boron signal was observed, the residue was washed repeatedly until the unreacted boron compound was not detectable by ^{11}B NMR spectroscopy.

Denaturation of Albumin-Polyhedral Borane Anion Complexes. Human serum albumin (HSA) (approximately 2 mg/mL) and the complex formed by the reaction of HSA and each of the polyhedral borane anions, designated as HSA-$B_{20}H_{17}SH$, HSA-$B_{20}H_{18}$, HSA-$B_{20}H_{17}OH$ were put in an 8 M urea solution. The samples were stored at 25 °C for 16 hours. The samples were transferred utilizing Pasteur pipettes to centricon YM-30 filters and filtered. Double distilled water (2.0 mL) was added, the sample was vortexed, and refiltered. The washing process was completed a total of three times. After the wash process was complete, the samples were transferred to clean vials marked in blue (control) and red (denatured). The samples were refrigerated until they could be prepared for analysis.

Glutathione Reaction. $Na_4B_{20}H_{17}SH$ (12.5 µl) was added to approximately 1.1 mg of both reduced and oxidized forms of glutathione. The reaction mixture was raised to a total volume of 100 µl in DI water. Unreacted solutions of both forms of glutathione were also made to act as controls. The solutions were allowed to react for 36 hours at a pH of approximately 7.36 in a water bath at a temperature of 37 °C.

An aliquot (10 µL) of each of the reaction mixtures was diluted to 200 µL in DI water and examined by capillary electrophoresis (CE) and HPLC. Both reduced and oxidized glutathione reaction material (50 pmol/µL) was run on the Beckman CE in H_2O. Approximately 1.1 mg of reduced and oxidized glutathione was weighed and placed in a 1.5 mL Eppendorf tube. Approximately 1100 µL of ultrapure H_2O was added and the solution vortexed to aid in solvation.

Instrumental Analysis

Description of Instrumentation. Instrumentation was located either at the Department of Chemistry and Biochemistry, Southwest Texas State University (San Marcos, TX), or the Department of Cellular and Molecular Biology, Protein Microanalysis Facility, University of Texas at Austin (Austin, TX).

Sodium Dodecyl Sulfate Polyacrylamide Gel Electrophoresis. Gel electrophoresis was performed on a NuPAGE 10%, Bis-Tris gel, in an Invitrogen Sure Lock II Mini Cell, using MOPS running buffer, LDS sample buffer, dithiothreitol (DTT), antioxidant and a VWR 105 power supply. The gels were run at 184 volts for an average of 30 minutes per run. Each experimental lane received 20 μL of sample while two lanes received Mark 12 standard. The gels were stained with colloidal blue stain.

Matrix Assisted Laser Desorption Ionization (MALDI) Mass Spectrometry. Measurements of protein masses were performed on a PerSeptive Biosystems Voyager MALDI-Time of Flight (TOF) mass spectrometer in the Protein Microanalysis Facility of the University of Texas at Austin. Protein samples in aqueous solution were combined with freshly prepared saturated sinapinic acid dissolved in a mixture of 50 % acetonitrile, 0.3% trifluoroacetic acid (TFA), and distilled water. Sample aliquots of 0.5 or 1.0 μL were spotted onto stainless steel sample plates and spectra were collected by averaging 10-20 laser shots. Samples were irradiated with a nitrogen laser (Laser Science Inc.) operated at 337 nm, and attenuated and focused on the sample target using the built-in software. Ions were accelerated with a deflection voltage of 30 kV. Ions were differentiated according to their m/z using a time-of-flight mass analyzer.

Capillary Zone Electrophoresis. Separation was achieved on a Beckman P/ACE System 5000 equipped with a P/ACE Diode Array Detector (PDA), a Beckman P/ACE Station software (version 4) in 50 mM sodium borate at a pH of 8.35. The column was a 75 μm x 57 cm capillary. The temperature was 22 °C for a series of twenty minute electrophoretic runs. The running voltage was 17.5 kV. Products were detected using UV detection at 214 nm.

UV-Visible Spectrophotometry (DTNB). Samples dissolved in 0.1 M phosphate buffered saline (PBS), at a pH of 8, were analyzed by uv-visible spectroscopy in a 1 cm quartz cell, at a read average time of 0.50 seconds. The samples were analyzed in the absorbance mode at 279, 412, and 530 cm^{-1}, on a Beckman DU-7400 uv-visible spectrometer. Five uv or visible wavelength evaluations were made for each sample and an average calculated.

High Performance Liquid Chromatography. Samples dissolved in water or reaction buffer were analyzed by reversed phase-HPLC. Whole proteins were analyzed on an AKTA HPLC using a Sephasil Peptide C8 column characterized as 0.46 cm x 5.0 cm. The flow rate was 0.5 mL/min on a 30 minute run utilizing a solvent gradient of 5 to 98%. Absorbance was monitored at 215 and 280 nm using a diode array detector. The trypsin digests were run on a Beckman System Gold HPLC with a Zorbax SBC18 (Separation Methods Technologies) column characterized as a 5 μm, 0.5 mm x 150 mm column. The flow rate was 0.040 mL/min on a 140 minute run utilizing a solvent gradient of 80% acetonitrile and 0.1% trifluoroacetic acid (TFA, buffer B). The column was kept at 55 °C. Absorbance was monitored at 214 and 280 nm using a diode array detector.

Sample Preparation. All protein-polyhedral borane anion reactions were performed in the Department of Chemistry and Biochemistry, Southwest Texas State University (San Marcos, TX) and transported, as necessary, to the Department of Cellular and Molecular Biology, University of Texas at Austin (Austin, TX). Samples for analysis on the instruments in the University of Texas facility were prepared in that facility. All other sample preparation was performed in the labs at Southwest Texas State University.

Sodium Dodecyl Sulfate Polyacrylamide Gel Electrophoresis. BSA solution (50 μL, 1 mg/mL) and solutions of BSA-$B_{20}H_{18}$, BSA-$B_{20}H_{17}OH$, BSA-$B_{20}H_{17}SH$ (50 μL, 1 mg/mL) were prepared. Two groups of samples were prepared for analysis. The first group of four samples was prepared using 50 μL of complex, 25 μL of ¼ dilute sample buffer, 10 μL of dithiothreitol, (DTT) and 15 μL of DI H_2O. The second group of samples was prepared identically except DTT was not added. A sample of each (20 μL) was loaded on a lane of a 10% Bis Tris Gel and run at 120 volts. The gels were subsequently stained with colloidal blue and imaged on a Kodak digital imager.

MALDI Mass Spectrometry Samples of BSA and the complexes that had been formed by the reaction of BSA and the three polyhedral borane anions, $[B_{20}H_{18}]^{2-}$, $[B_{20}H_{17}OH]^{4-}$, $[B_{20}H_{17}SH]^{4-}$, were prepared for analysis by MALDI Mass Spectrometry. BSA and each of the BSA boron complexes (1 mg/mL) in DI H_2O was diluted 1:10 in DI H_2O. Although mass spectral measurements were made with ratios of protein, or protein complex, with sinapinic acid ranging from 1:1 to 1:6, the optimum ratio was typically 1:4. All reported spectra were made with a ratio of 1:4.

Capillary Zone Electrophoresis Reduced and oxidized glutathione (1.08 mg, 0.00351 mol and 1.13 g, 0.00184 mol respectively) was diluted in 1.08 mL and 1.13 mL of ultrapure H_2O respectively. A 1:100 dilution was made and 200 pmol run on the Beckman P/ACE CZE.

UV-Visible Spectrophotometry (DTNB) Six serial dilutions were completed by adding 0.10 M PBS to a BSA solution with a concentration of 3.5×10^{-5} M. The resulting solutions had concentrations of 3.00×10^{-5} M, 2.50×10^{-5} M, 2.00×10^{-5} M, 1.50×10^{-5} M, 1.00×10^{-5} M, 5.00×10^{-6} M. The seven total samples were analyzed with a uv-visible spectrometer and a Beer's Law plot was completed.

A stock solution of DTNB was prepared by adding 39.6 mg DTNB to 10 mL of 0.1 M PBS. The pH was raised to 8.0 by addition of 0.1 M NaOH. A blank consisting of 1 mL of the PBS solution was used to zero the uv-vis spectrometer. All of the samples were numbered 1-4 starting with the unreacted BSA and proceeding through the three different BSA-boron complexes. The sample of unreacted BSA in PBS was analyzed with the uv-vis spectrometer at 280 nm and 412 nm to determine the concentration of BSA and a reference for calculating the thiolate anion concentration. Each BSA-boron complex solution was examined with the uv-vis spectrometer to determine the concentration of the BSA-boron complex and the reference for DTNB. Once the absorbance of each sample in the absence of DTNB had been determined, 20 μL of DTNB was added to the blank and a reading was taken at 280 and 412 nm. Next 20 μL of DTNB was added to sample number one, the unreacted BSA, and a reading taken at 280 and 412 nm at time intervals starting at 3 minutes and proceeding until the

absorbance at 412 nm became stable. The procedure was repeated for each sample of BSA-boron complex.

High Performance Liquid Chromatography. The 2 mg/mL samples of HSA, HSA-$B_{20}H_{17}SH$, HSA-$B_{20}H_{18}$, HSA-$B_{20}H_{17}OH$ were spun down on a centrifuge at 10K rpm for two minutes. An aliquot of the supernatant from each sample (25 μL) was diluted to 100 μL with DI water bringing the approximate concentration to 0.5 mg/mL. Each sample was subsequently diluted again 1:4 to approximately 0.1 mg/mL. An aliquot of each of these samples (10 μL) was diluted to 100 μL with buffer A (0.1% TFA) and evaluated by HPLC.

Samples of HSA, HSA-$B_{20}H_{17}SH$, HSA-$B_{20}H_{18}$, HSA-$B_{20}H_{17}OH$ (25 μL) at a concentration of 0.5 mg/mL were diluted to 100 μL in DI water and were brought to a pH of 8 with Tris. Trypsin was added to each sample at a ratio of 1:50, Trypsin:HSA. The samples were vortexed and placed in a 37 °C sand bath for 48 hours. The samples were removed from the sand bath and frozen to stop the digestion. Each sample was later warmed to room temperature and centrifuged at 9000 rpm for 4 minutes. An aliquot of the supernatant (20 μL) was diluted to 100μL with DI water. Each of these (10 μL) samples was diluted to 100 μL with buffer A (0.1 % TFA) and evaluated by HPLC.

CHAPTER 4

RESULTS AND DISCUSSION

Compound Selection and Synthesis

Three polyhedral borane anions, $[B_{20}H_{18}]^{2-}$, $[B_{20}H_{17}OH]^{4-}$, and $[B_{20}H_{17}SH]^{4-}$, were selected for investigation based on the reported *in vivo* biodistribution results.[20,21] The $[B_{20}H_{18}]^{2-}$ anion, encapsulated in unilamellar liposomes, was retained in the tumor to a large extent in the murine biodistribution experiment. The $[B_{20}H_{17}OH]^{4-}$ anion, encapsulated in unilamellar liposomes, was cleared from all tissues, including tumor, in the murine biodistribution experiment. The $[B_{20}H_{17}SH]^{4-}$ anion, also encapsulated in unilamellar liposomes, was accreted in the tumor in murine biodistribution experiments. The retention of $[B_{20}H_{18}]^{2-}$ and the accretion of $[B_{20}H_{17}SH]^{4-}$ has been attributed to the formation of covalent bonds with intracellular protein moieties.[20,21]

The synthesis of each polyhedral borane anion was completed using known procedures.[23,35-37] The starting material for each of the three was $(Et_3NH)_2[B_{10}H_{10}]$, prepared by the reaction of decaborane, $B_{10}H_{14}$, and triethylamine, Et_3N (Reaction 1).[36]

$$B_{10}H_{14} + 2\,Et_3N \rightarrow (Et_3NH)_2B_{10}H_{10} + H_2 \qquad (1)$$

Recrystallization of the crude product from a water/ethanol mixture produced the white crystalline product in 74 % yield. The identity of the product was confirmed by ^{11}B NMR spectroscopy.

The triethylammonium cation was removed by the reaction of an aqueous solution

of $(Et_3NH)_2[B_{10}H_{10}]$ with an excess of sodium hydroxide to produce the sodium salt of the $[B_{10}H_{10}]^{2-}$ anion (Reaction 2). The $[B_{10}H_{10}]^{2-}$ anion does not react with

$$(Et_3NH)_2[B_{10}H_{10}] + 2\,NaOH \rightarrow Na_2[B_{10}H_{10}] + 2\,Et_3N + 2\,H_2O \qquad (2)$$

nucleophiles such as the hydroxide anion and is stable in the basic solution. Acidification of the solution was required prior to the subsequent reaction since the $[B_{20}H_{18}]^{2-}$ anion will react with the hydroxide ion.[35]

Oxidation of the $[B_{10}H_{10}]^{2-}$ ion with ferric ion produces the coupled species, $[B_{20}H_{18}]^{2-}$ (Reaction 3).[37] The sodium cation of the $[B_{10}H_{10}]^{2-}$ starting material is also

$$Na_2[B_{10}H_{10}] + 2\,FeCl_3 \rightarrow Na_2[B_{20}H_{18}] + 2\,FeCl_2 + 2\,HCl \qquad (3)$$

the counterion for the product. The isolation of the $[B_{20}H_{18}]^{2-}$ ion was accomplished by precipitation of the anion by addition of an aqueous solution of cesium chloride, CsCl (Reaction 4). The $Cs_2[B_{20}H_{18}]$ product was isolated in a 83 % yield by recrystallization from boiling water.

$$Na_2[B_{20}H_{18}] + 2\,CsCl \rightarrow Cs_2[B_{20}H_{18}] + 2\,NaCl \qquad (4)$$

The formation of the protonated form, $(H_3O)_2[B_{20}H_{18}]$, is accomplished on an anion exchange column. The protonated form is desired since the amount of the species can be determined by titration of the protonated form with a standardized solution of

NaOH. Removal of the solvent after the titration and dissolution of the solid in water using a volumetric flask produced the $Na_2[B_{20}H_{18}]$ solution with a known concentration. The identity of the product was confirmed by ^{11}B NMR spectroscopy (Figure 10).

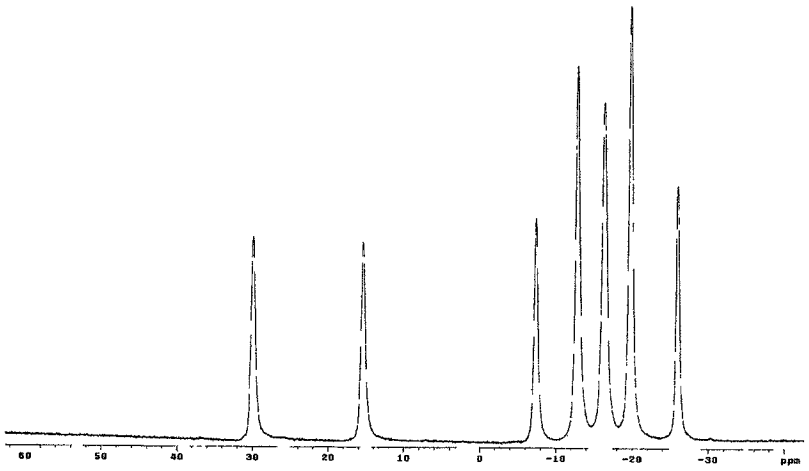

Figure 10: $\{^1H\}^{11}B$ NMR spectrum of $Na_2[B_{20}H_{18}]$

The sodium salt of the $[B_{20}H_{17}OH]^{4-}$ was produced by the reaction of hydroxide ion $[OH]^-$ with $Na_2[B_{20}H_{18}]$ (Reaction 5).[35] The $[B_{20}H_{18}]^{2-}$ ion is characterized by the presence of two three-center, two-electron bonds. The electron-deficient bonding region is susceptible to nucleophilic attack. Two equivalents of the nucleophile are required to

$$Na_2[B_{20}H_{18}] + 2\ NaOH \rightarrow Na_4[B_{20}H_{17}OH] + H_2O \qquad (5)$$

deprotonate the intermediate in the reaction sequence, $[B_{20}H_{18}OH]^{3-}$. The kinetic isomer is characterized by an apical-equatorial intercage connection. Rearrangement to the thermodynamic isomer, characterized by an apical-apical intercage connection, is

catalyzed by the presence of acid (Reaction 6).[35] Therefore, the thermodynamic isomer was prepared by dissolving the kinetic isomer in acid, followed by the addition of NaOH to remove the bridge proton.

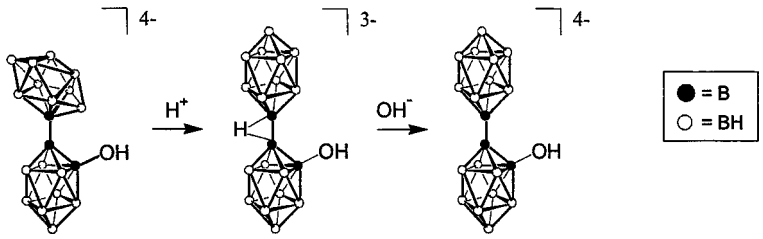

(6)

The potassium salt, $K_4[B_{20}H_{17}OH]$ was isolated by the addition of a saturated solution of potassium acetate in ethanol and recrystallized from water/ethanol to form the product in 94 % yield. The potassium salt was ion-exchanged to the protonated form which was then titrated with standardized base to produce the sodium salt as performed earlier with the $Na_2[B_{20}H_{18}]$. The compound was characterized by ^{11}B NMR spectroscopy. The ^{11}BNMR spectrum of the product (Figure 11) at pH 7.4 displayed peaks corresponding to the apical-equatorial isomer and the apical-apical isomer. There is no known difference in reactivity between the two.

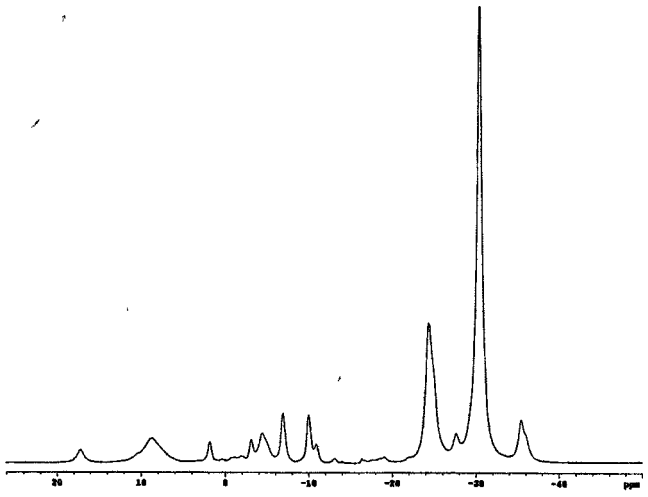

Figure 11: $\{^1H\}^{11}B$ NMR of $Na_4[B_{20}H_{17}OH]$

The Bender's salt, $KSC(O)OC(CH_3)_3$, was prepared by published methods.[38] The reaction of the Bender's salt and $(Et_3NH)_2[B_{20}H_{18}]$ at room temperature in tetrahydrofuran produces the protected thiol anion, $[B_{20}H_{17}SC(O)OC(CH_3)_3]^{4-}$, in good yield (Reaction 7).[23] The triethylammonium salt of the $[B_{20}H_{18}]^{2-}$ is prepared by the

$$(Et_3NH)_2[B_{20}H_{18}] + 4\,KSC(O)OC(CH_3)_3 \rightarrow$$
$$K_4[B_{20}H_{17}SC(O)OC(CH_3)_3] + 3\,HSC(O)OC(CH_3)_3 + 2\,Et_3N \qquad (7)$$

direct oxidation of $(Et_3NH)_2[B_{10}H_{10}]$ and subsequent recrystallization of the product from boiling water. The intermediate was characterized by ^1H, ^{13}C, and ^{11}B NMR. During characterization, the presence of four additional peaks in the ^{13}C NMR was noted. The impurity is present in small amount and is believed to be the result of ring-opening of the tetrahydrofuran solvent and subsequent nucleophilic attack to form the $[B_{20}H_{17}OCH_2CH_2CH_2CH_3]^{4-}$ anion. The impurity is present throughout the reaction sequence, but the small amounts should not alter any of the analytical results. Deprotection of the intermediate with acid, followed by basification with NaOH to remove the bridge proton, yields the $[B_{20}H_{17}SH]^{4-}$ anion (Reaction 8). The product of

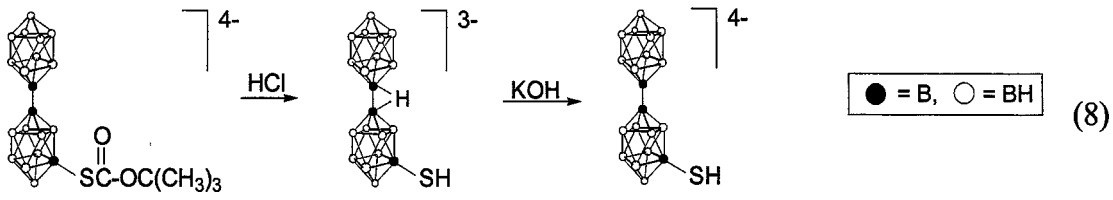

(8)

the reaction, $K_4[B_{20}H_{17}SH]$ is recrystallized from water/ethanol. The identity of the

product was confirmed by ^{11}B NMR (Figure 12). The ^{11}B NMR displays the equilibrium mixture between $[B_{20}H_{17}SH]^{4-}$ and $[B_{20}H_{18}SH]^{3-}$. The compound was ion-exchanged directly to the sodium salt and the concentration determined by the amount of product eluted through the column.

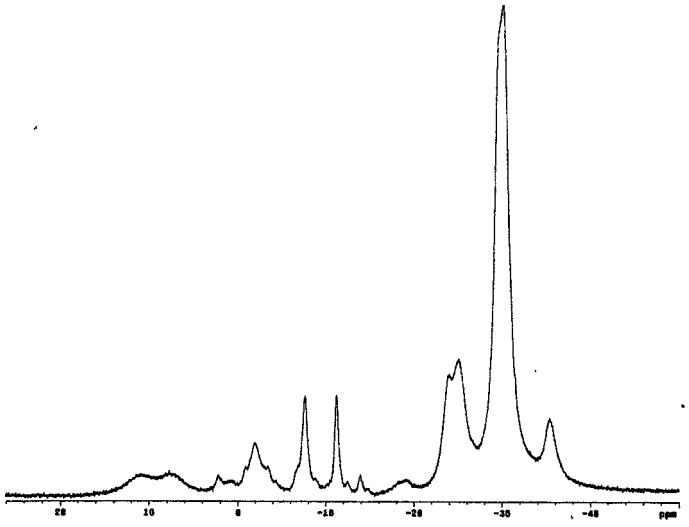

Figure 12: $\{^1H\}^{11}B$ NMR of $Na_4[B_{20}H_{17}SH]$

Selection of Bovine Serum Albumin

Serum albumin is one of the most commonly used and well-characterized proteins in scientific research. As one of the most abundant proteins in plasma, serum albumin is very inexpensive and relatively easy to purify making it a popular choice amongst a host of researchers. Over the years many have studied the structure and properties of serum albumin and determined how it interacts with other proteins, metals, carbohydrates, lipids and pharmaceuticals in a variety of conditions.[39]

The amino acid composition of bovine serum albumin is characterized by a high content of cysteines and the charged amino acids aspartic and glutamic acid, lysine and

arginine. In bovine serum albumin, the content of glycine, isoleucine, tryptophan, and methionine are lower than the average protein.[40]

Amino Acid Composition of BSA							
Alanine	48	Cysteine	35	Aspartate	41	Glutamate	58
Phenylalanine	30	Glycine	17	Histidine	16	Isoleucine	15
Lysine	60	Leucine	65	Methionine	5	Asparagine	14
Proline	28	Glutamine	21	Arginine	26	Serine	32
Threonine	34	Valine	38	Tryptophan	3	Tyrosine	21

Table 3: Amino acid composition of BSA

There are 17 protected, interchain disulfide bonds in BSA that are not readily available to solvents at a neutral pH. The combination of nucleophilic sites and the single, well characterized, free sulfhydryl (SH) group on cysteine 34 make BSA an attractive protein for investigation. The molecular weight of the powdered BSA obtained from Sigma Aldrich is listed as 66,430 daltons based on the amino acid sequence. BSA is constructed from a single polypeptide chain with no carbohydrates. The pI in water at 25 °C is approximately 4.7 to 4.9. The maximum absorption in a UV spectrum is 279-280 nm and the extinction coefficient is 39,080 M^{-1} cm^{-1}.[41]

Results with Bovine Serum Albumin

Sodium Dodecyl Polyacrylamide Gel Electrophoresis. The initial strategy for the detection of the presence of covalent bonds between the polyhedral borane anions and BSA was to examine the molecular weight of the control BSA sample and compare it to the three samples which resulted from the reaction of BSA and each of the polyhedral

borane anions. Theoretically, if covalent bonds had formed between the BSA and the polyhedral borane anion, there would be an increase in molecular weight proportional to the number of anions that had bound to the BSA.

Sodium dodecyl sulfate-polyacrylamide gel electrophoresis (SDS-PAGE) was selected as a relatively simple, well known, technique that can separate the components of a protein mixture based on mass. Any BSA that had reacted with one or more of the polyhedral borane anions should exhibit a higher molar mass and the difference in mass could be observable on the stained gel.

Each of the polyhedral borane anions was allowed to react with the BSA under physiological conditions. The reactions were performed in phosphate-buffered saline at a temperature of 37 °C for a period of 36 hours. The unreacted polyhedral borane anions were separated from the reaction product by repeated washing and filtration through Centricon-30 filters. The washing process was repeated until no free boron compound was evident in the ^{11}B NMR spectrum of the sample. The products of the reaction were reconstituted in ultra-pure water and prepared for SDS-PAGE according to the standard protocol produced by Invitrogen for a 10% Bis-Tris precut gel.

Once the gel electrophoresis was complete, the gel was stained with colloidal blue, photographed and analyzed with the Kodak imager. Molecular weight determinations were completed by the imager based on the Mark 12 standard (Figure 13).

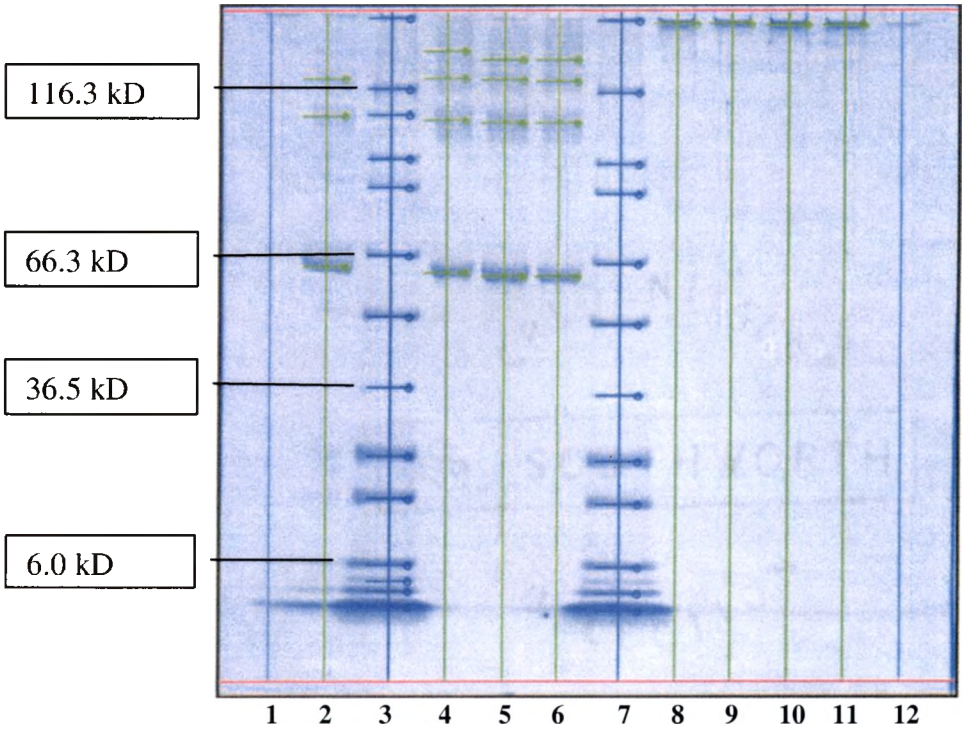

Figure 13: SDS-PAGE of BSA and the products of the reaction of BSA and the polyhedral borane anions. Lane 1: Empty, Lane 2: BSA reduced., Lane 3: Mark 12 Standard, Lane 4: BSA-$B_{20}H_{18}$ reduced., Lane 5: BSA-$B_{20}H_{17}OH$-reduced, Lane 6: BSA-$B_{20}H_{17}SH$-reduced, Lane 7: Standard, Lane 8: BSA, Lane 9: BSA-$B_{20}H_{18}$, Lane 10: BSA-$B_{20}H_{17}OH$, Lane 11: BSA-$B_{20}H_{17}SH$, Lane 12: Empty

Since the sodium dodecyl sulfate effectively disrupts most non-covalent bonds, any associations that are non-covalent should not be present on the gel. Any difference in mass indicated by the band location would theoretically be due to the presence of a covalent modification to the protein. The distinctions between bands on the resulting gel are so small as to fall within what one would expect for minor fluctuations in the normal movement of a given analyte through the polyacrylamide gel. Since no modification of the BSA could be observed as a consequence of the formation of a covalent bond between any of the polyhedral borane anions and the protein, either there is no covalent modification of the BSA by any of the polyhedral borane anions or the modification is not detectable due to the poor resolution of the technique.

The samples were evaluated without reduction by DTT (Lanes 9-11) in order to avoid the possibility of reducing the disulfide bond that might have formed between the sulfhydryl group on $Na_4[B_{20}H_{17}SH]$ and the free thiol on cysteine 34 of BSA. Without DTT, internal disulfide bonds between cysteine residues remain intact and a complete unfolding of the protein does not occur. As a result, the protein in this case did not move through the gel, but merely sat at the top of the well. While there are protocols for performing gel electrophoresis without disulfide reduction, the results of lanes 2-5 indicated that a technique with greater resolution was required to detect the small mass differences that might be occurring as a result of any covalent modification.

MALDI Mass Spectrometry. MALDI-TOF mass spectrometry was employed to determine the mass differences between BSA and the product of the reaction between BSA and each of the three polyhedral borane anions under investigation (Figure 14). Each of the four samples was analyzed several times for the purpose of acquiring a statistical average and a standard deviation (Table 4).

Sample	Average m/z	Standard Deviation	Average Difference with control (BSA)	Approximate Number of Bound Polyhedral Borane Anions
BSA	66,336	122	0	0
BSA-$B_{20}H_{18}$	68,078	522	1,742	~6
BSA-$B_{20}H_{17}OH$	67,579	182	1,243	~4
BSA-$B_{20}H_{17}SH$	69,332	625	2,996	~8

Table 4: MALDI-MS of BSA and the products of the reaction between BSA and the polyhedral borane anions

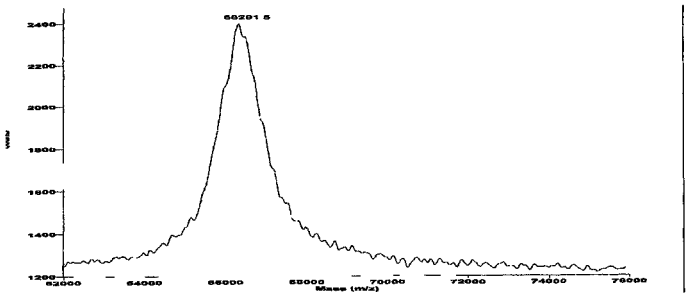

Unreacted BSA

MW = 66292 Daltons

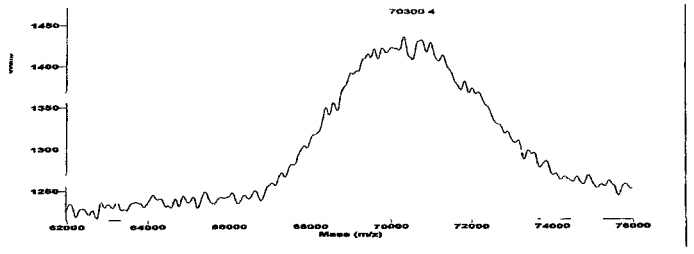

BSA-$B_{20}H_{18}$

MW = 70300 Daltons

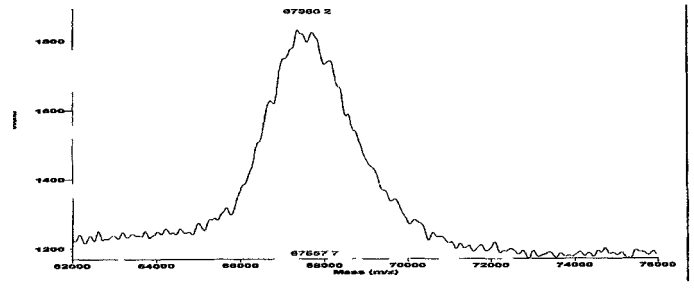

BSA-$B_{20}H_{17}OH$

MW = 67380 Daltons

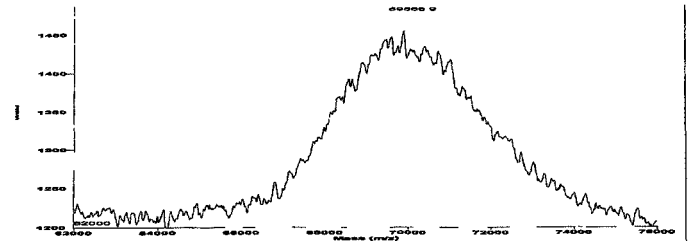

BSA-$B_{20}H_{17}SH$

MW = 69869 Daltons

Figure 14: MALDI-MS spectra of BSA and the products of the reaction of BSA and the polyhedral borane anions

BSA has a molecular weight of approximately 66 kD while the molecular weight of the polyhedral borane compounds range from 280-358 D. Based on previous biodistribution data and the known chemical reactivity of the polyhedral borane anions, it was anticipated that the $[B_{20}H_{18}]^{2-}$ and $[B_{20}H_{17}SH]^{4-}$ anions would react with the BSA while the $[B_{20}H_{17}OH]^{4-}$ anion would not react with BSA. The extensive washing and filtering process that was completed for each sample should have removed any compound that had not been tightly bound to the protein. Although the increase in molecular weight is more substantial for the $[B_{20}H_{18}]^{2-}$ and $[B_{20}H_{17}SH]^{4-}$ anions, the MALDI data indicates an increase in the molecular weight for all of the reaction products.

The shift in the mass to charge ratio indicates a change in molecular weight, but the increased broadness observed in the BSA-$B_{20}H_{18}$ and the BSA-$B_{20}H_{17}SH$ spectra is also significant. The data may suggest that tight, non-covalent interactions are present or that the complex has more than one type of covalent bond present in more than one location. Since the chemistry of the polyhedral borane anions has been thoroughly investigated and the potential binding sites are well understood, the possibility of tight, non-covalent interactions must be considered.

UV-Visible Spectrophotometry (DTNB). A standard technique,[42] based on the chemistry of 5,5-dithiobis(2-nitrobenzoic acid) [DTNB], commonly referred to as Ellman's Reagent, was utilized for the measurement of available cysteine residues on the protein. Ellman's Reagent contains a disulfide bond. That bond will react with an available cysteine thiol residue (Figure 15), subsequently releasing a thiolate anion. The thiolate anion is highly colored and absorbs at 412 nm. The unreacted BSA and the products resulting from the reaction of BSA and each of the three polyhedral borane

anions were evaluated. For BSA, cysteine 34 provides the only available sulfhydryl group. Therefore, reaction of Ellman's reagent and BSA would result in a concentration of thiolate ion equal to that of the BSA.

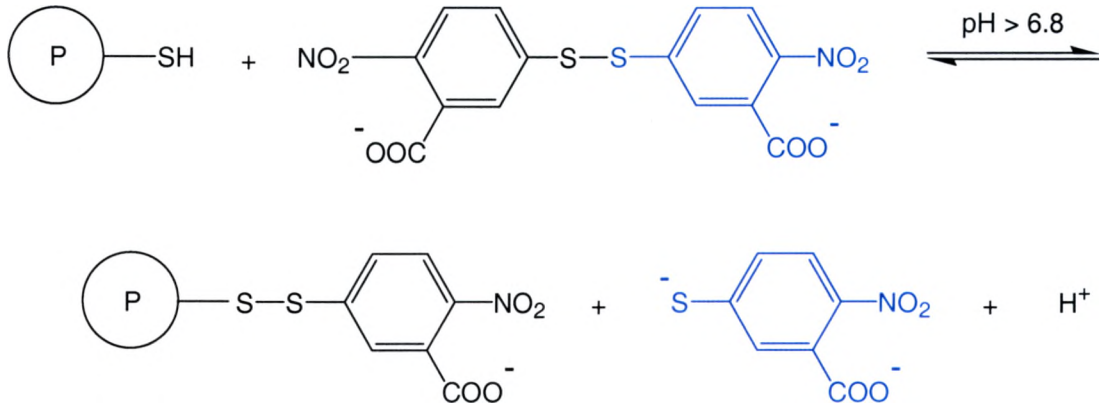

Figure 15: Reaction of DTNB and a thiol residue on a protein

The maximum absorbance of the protein was determined to be 279 nm. A concentration calibration curve (Figure 16) was constructed based on six concentrations of pure BSA. The slope of the line was determined by linear best-fit analysis to be

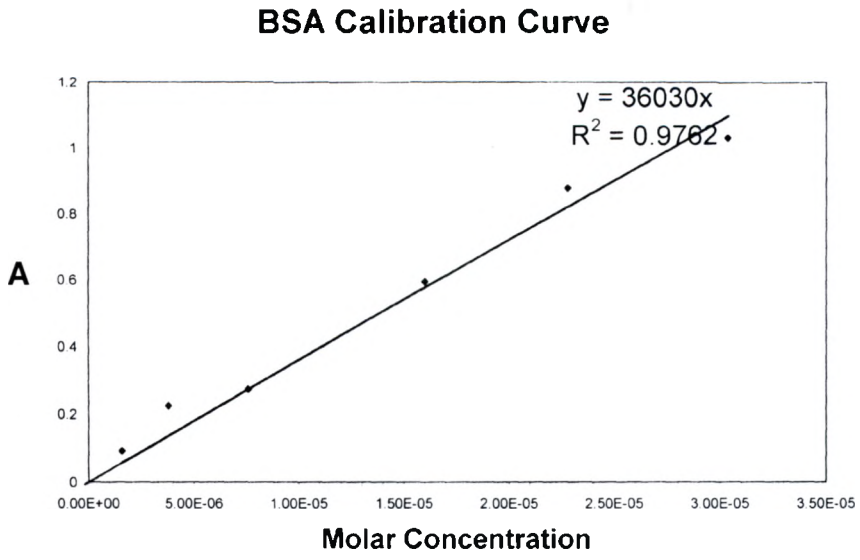

Figure 16: Calibration curve for BSA

36,030 M^{-1} cm^{-1} with a R^2 correlation of 0.9762. The extinction coefficient for BSA is equivalent to the slope of the line. The literature value of the extinction coefficient for BSA is 39,080 M^{-1} cm^{-1}.[41] The BSA concentration for each of the trials was determined from the calibration curve. The absorption of the protein was also measured at 412 nm, the maximum absorbance associated with the thiolate anion. The absorption at 412 nm is used as the baseline reading for the concentration of the thiolate anion.

When the DTNB was added to the BSA, an observable color change was produced. The absorption at 412 nm was measured to determine the concentration of the thiolate anion. The literature value of the extinction coefficient for the thiolate anion, 13,600 M^{-1} cm^{-1}, was used.[42] During the experiment, five consecutive measurements were made at 279 nm and 412 nm and the average of the five measurements was used in the calculations. The concentration of the BSA represents the concentration of free sulfhydryl groups since only one free sulfhydryl group is present in BSA. Therefore, the number of free sulfhydryl groups was determined by calculating an average absorbance of the BSA at 279 nm and dividing the absorbance by the extinction coefficient, 36,030 M^{-1} cm^{-1}. The thiolate anion concentration was determined by subtracting the average for the reference absorbance at 412 nm from the average absorbance at 412 nm after the addition of DTNB and dividing that by the extinction coefficient for the thiolate anion 13,600 M^{-1} cm^{-1}. By dividing the resulting concentration for the thiolate anion by the concentration for the BSA, a ratio is obtained that indicates the relative concentration of sulfhydryl groups available on BSA. Since BSA has only one free sulfhydryl group, the ratio of these two concentrations should be equal to one.

The only polyhedral borane anion investigated that should, based on the known

chemistry, form a disulfide bond with BSA is the $[B_{20}H_{17}SH]^{4-}$ anion (Figure 8). Consequently, if the free cysteine residue on BSA is no longer available due to the formation of a disulfide bond with the thiol on the polyhedral borane anion, then DTNB will be unable to form a disulfide bond with the protein. As a result of this covalent bond there will be no increase in absorbance at 412 nm from the release of a thiolate anion when DTNB is added to the solution. Alternatively, if the polyhedral borane anion does not react with the cysteine residue on BSA, the protein will react with the DTNB analogous to the unreacted BSA. Therefore, the value of the ratio for the $[B_{20}H_{17}SH]^{4-}$ should theoretically be zero and the value of the ratio for the $[B_{20}H_{18}]^{2-}$ and $[B_{20}H_{17}OH]^{4-}$ should theoretically be one.

The results of the DTNB experiments are depicted in Table 5. In each case, the value of the concentration ratio has been normalized by dividing by the value obtained for unreacted BSA to produce a value of one for BSA. The value for BSA is 1.0 from the normalization process while the average value for the $[B_{20}H_{17}SH]^{4-}$ anion is 0.08 ±0.05, the average value for the $[B_{20}H_{18}]^{2-}$ anion is 0.40 ± 0.11 , and the average value for the $[B_{20}H_{17}OH]^{4-}$ is 0.65 ± 0.26. Although the value obtained for the $[B_{20}H_{17}SH]^{4-}$ is as predicted, the other two polyhedral borane anions deviated from the theoretical values.

	BSA	BSA-$B_{20}H_{18}$	BSA-$B_{20}H_{17}OH$	BSA-$B_{20}H_{17}SH$
Experiment 1	1	0.28	0.88	0.04
Experiment 2	1	0.47	0.86	0.07
Experiment 3	1	0.51	0.34	0.03
Experiment 4	1	0.35	0.53	0.15
Average	1	0.40	0.65	0.08
Standard Deviation	0	0.11	0.26	0.05

Table 5: Ratios of the concentration of protein to the concentration of free thiolate ion in solution after the addition of DTNB

The $[B_{20}H_{18}]^{2-}$ anion might be expected to react with the free thiol on BSA since the free thiol may be a relatively weak nucleophile. Consequently, less absorbance may be observed at 412 nm due to the production of a covalent bond between the polyhedral borane anion and the thiol residue. A similar analogy cannot be drawn with the $[B_{20}H_{17}OH]^{4-}$ anion since the anion is known to be unreactive at physiological conditions.

Results with Human Serum Albumin

Comparison to Bovine Serum Albumin. Dr. Klaus Linse (Department of Cellular and Molecular Biology, Protein Microanalysis Facility, University of Texas at Austin) recommended the utilization of human serum albumin (HSA) for future investigations. The basis for the recommendation was the chemical resemblance between HSA and BSA with the added advantage of being a plasma protein obtained from human tissue.

The resemblance between the two serum albumins was supported by the literature. The amino acid composition (Table 6) is similar to that of BSA.[43] In addition,

Amino Acid Composition of HSA							
Alanine	63	Cysteine	35	Aspartate	39	Glutamate	60
Phenylalanine	30	Glycine	12	Histidine	16	Isoleucine	8
Lysine	58	Leucine	61	Methionine	6	Asparagine	15
Proline	25	Glutamine	23	Arginine	23	Serine	22
Threonine	30	Valine	39	Tryptophan	1	Tyrosine	18

Table 6: Amino acid composition of HSA

numerous articles regarding drug binding,[44] homocysteine levels in blood,[39] and the binding of different metals such as La^{3+}, Cu^{2+}, Zn^{2+} utilize HSA and BSA interchangeably.[45] Japanese researchers, Moriyama and Takeda, investigated a direct comparison in the reformation of the helical structure of the two serum albumins after denaturing the proteins with urea.[46] While there were differences in the reformation of α-helical structure, the intact proteins possess only a 1% difference in α-helicity at pH 7. Both possess 17 internal disulfide bonds and a free sulfhydryl group at cysteine 34.[39] In addition, both HSA and BSA remain essentially in their native secondary structure when the sulfhydryl group is modified.[39]

MALDI Mass Spectrometry. As with BSA, MALDI-TOF mass spectrometry was utilized to determine the molecular weight of the HSA as well as the products formed by the reaction of HSA and the polyhedral borane anions (Figure 17). The MALDI mass spectra were obtained using samples prepared as for BSA. Each of the four samples was analyzed several times for the purpose of acquiring a statistical average and a standard deviation (Table 7). The results obtained with HSA, particularly when the standard deviations are considered, are quite similar. The

Analyte	Average m/z	Standard Deviation	Average Difference with control (HSA)	Possible Number of Polyhedral Borane Anions
HSA	67,148	258	0	0
HSA-$B_{20}H_{18}$	69,545	133	2397	~8
HSA-$B_{20}H_{17}OH$	67,846	394	698	~2
HSA-$B_{20}H_{17}SH$	69,185	151	2037	~6

Table 7: MALDI-MS of HSA and the products of the reaction between BSA and the polyhedral borane anions

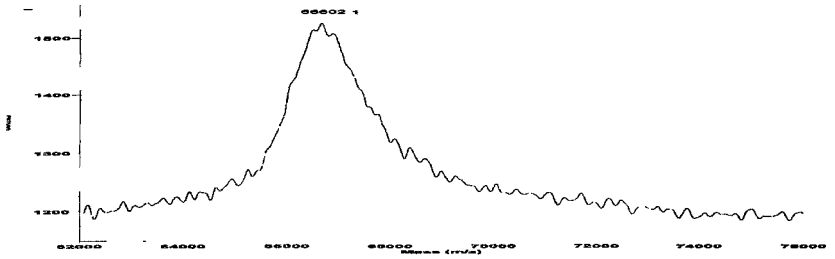

Unreacted HSA

MW = 66602 kD

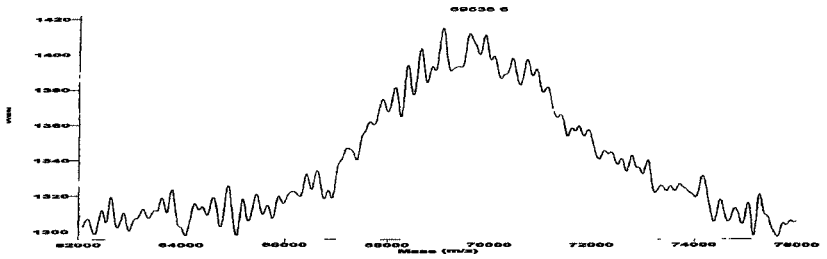

$HSA\text{-}B_{20}H_{18}$

MW = 69538 kD

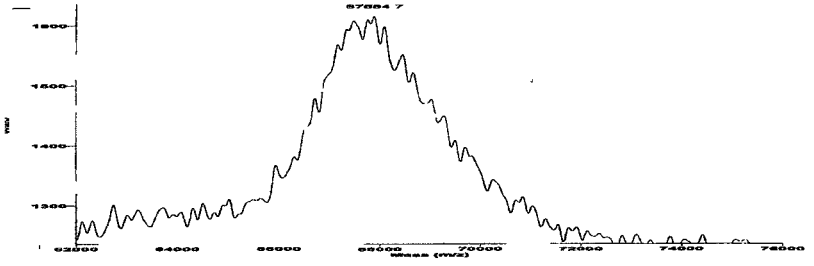

$HSA\text{-}B_{20}H_{17}OH$

MW = 67684 kD

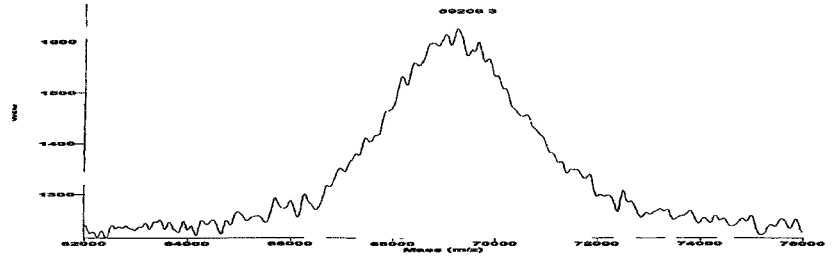

$HSA\text{-}B_{20}H_{17}SH$

MW = 69208 kD

Figure 17: MALDI-MS spectra of HSA and the products of the reaction of HSA and the polyhedral borane anions

molecular weight of the polyhedral borane compounds range from approximately 280-358 D. The results indicate that the molecular weight increases more with the $[B_{20}H_{18}]^{2-}$ and the $[B_{20}H_{17}SH]^{4-}$ anions than with the $[B_{20}H_{17}OH]^{4-}$ anion, as observed for BSA.

The MALDI data indicates that all of the compounds interact to some degree. Similar to BSA, the molecular weight shift is accompanied by an increase in the broadness of the signal, particularly with the HSA-$B_{20}H_{18}$ and HSA-$B_{20}H_{17}SH$ products. The data suggests that there may be bound anions for these two complexes in a number of different locations and that the peaks represent more than one species of HSA polyhedral borane anion complex. Based on the known reactivity of the polyhedral borane anions and the rigorous washing protocol applied to the samples prior to analysis, tight ionic interactions are suspected, particularly in the case of the $[B_{20}H_{17}OH]^{4-}$ anion. The possibility of a covalent bond formed by a mechanism other than previously described cannot be completely excluded from future inquiry; however, boron chemists consider this to be unlikely.

If the interaction between the HSA and the polyhedral borane anions is electrostatic in nature, removal of the non-covalently attached species should be facilitated by the interruption of the secondary structure of the HSA followed by repeated washing to remove the unbound ionic species. Urea is a common denaturant utilized to disrupt the hydrogen bonding within proteins.[46] Therefore, the product of the reaction between HSA and each of the polyhedral borane anions was treated with 8 M urea, followed by repeated washing with DI water to remove excess compound and excess urea. The residue remaining after the denaturing process was reconstituted in water and evaluated by MALDI mass spectrometry.

The denatured samples did not ionize well, possibly as a result of the lower concentration of the sample resulting from the increased number of washings. Increased laser intensities did not enhance the results and large signal to noise ratios were observed in all of the mass spectra (Figure 18). Further attempts at sample analysis by MALDI were terminated owing to time considerations and the needs of other users.

Of the four samples analyzed, the unreacted HSA control and the HSA complexed with the $[B_{20}H_{17}SH]^{4-}$ anion were the most readable. The shift in mass to charge ratio between HSA and HSA-$B_{20}H_{17}SH$ did not reflect a significant change as a result of the denaturation process. The mass equivalent of three $[B_{20}H_{17}SH]^{4-}$ anions has been removed suggesting that some of the compound was electrostatically bound to the protein and was removed in the urea wash. An average mass and standard deviation could not be obtained since only one measurement was completed. The other two complexes produce relatively poor spectra and may be an unreliable source of numerical data as far as their mass to charge ratios. They are, however, included for the purpose of comparison.

The purpose of the treatment of the samples with 8 M urea was to facilitate the removal of any non-covalently bound polyhedral borane anions. While there is an indication that a small amount of electrostatically bound compound may have been removed from the protein, there is no adequate explanation for the observed large increase in molecular weight. Consultation with authorities and references on boron chemistry were unable to understand how this empirical result could be anything other than an electrostatic interaction initiated by the large delocalized negative charge on the boron cages.

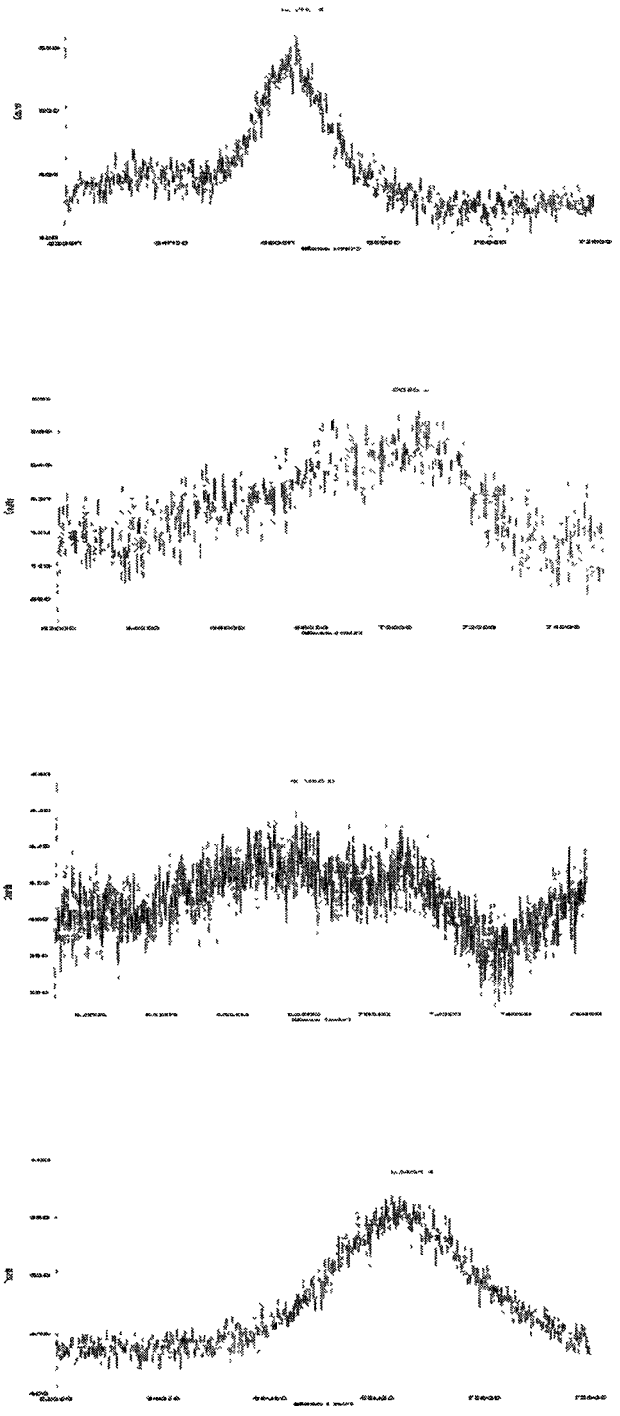

Figure 18: MALDI-MS spectra of denatured HSA and the products of the reaction of HSA and the polyhedral borane anions

Capillary Zone Electrophoresis. Capillary zone electrophoresis (CZE) was employed to investigate changes in the electronic environment of HSA once the reaction protocol with the polyhedral borane anions was completed. In CZE, an applied electric field creates the electroosmotic flow that moves from the positive to the negative terminal in a fused silica capillary. The bulk flow carries all species in the same direction at migration rates that vary according to the degree that the species are negative or positive and the resistance to the mass of the species. The more positively charged molecule will migrate faster, followed by neutral species, and then the negatively charged species. The larger molecules require a greater force to overcome the greater mass of the larger molecule.

All of the signals corresponding to the product of the reaction between HSA and the polyhedral borane anions are broad and slightly shifted when compared to HSA (Figure 19); however, the most notable shift occurs in the HSA-$B_{20}H_{17}SH$ complex. The observable peak broadening may be attributed to the existence of complexes which differ by only one polyhedral borane anion. The shift of the signal for the HSA-$B_{20}H_{17}SH$ complex is 20 seconds and for the other two complexes, the shift is considerably less. The difference in mass between the HSA (66 kD) and the HSA-polyhedral borane anion complexes is relatively small. Therefore, the effect of the change in mass is small and could account for the small shift in the signal. Additionally, the effect of the increased charge on the protein as a result of the bound polyhedral borane anion is diminished due to delocalization of the charge over the entire protein. Although the results of the CZE investigation indicate that some type of binding has occurred, the nature of the interaction

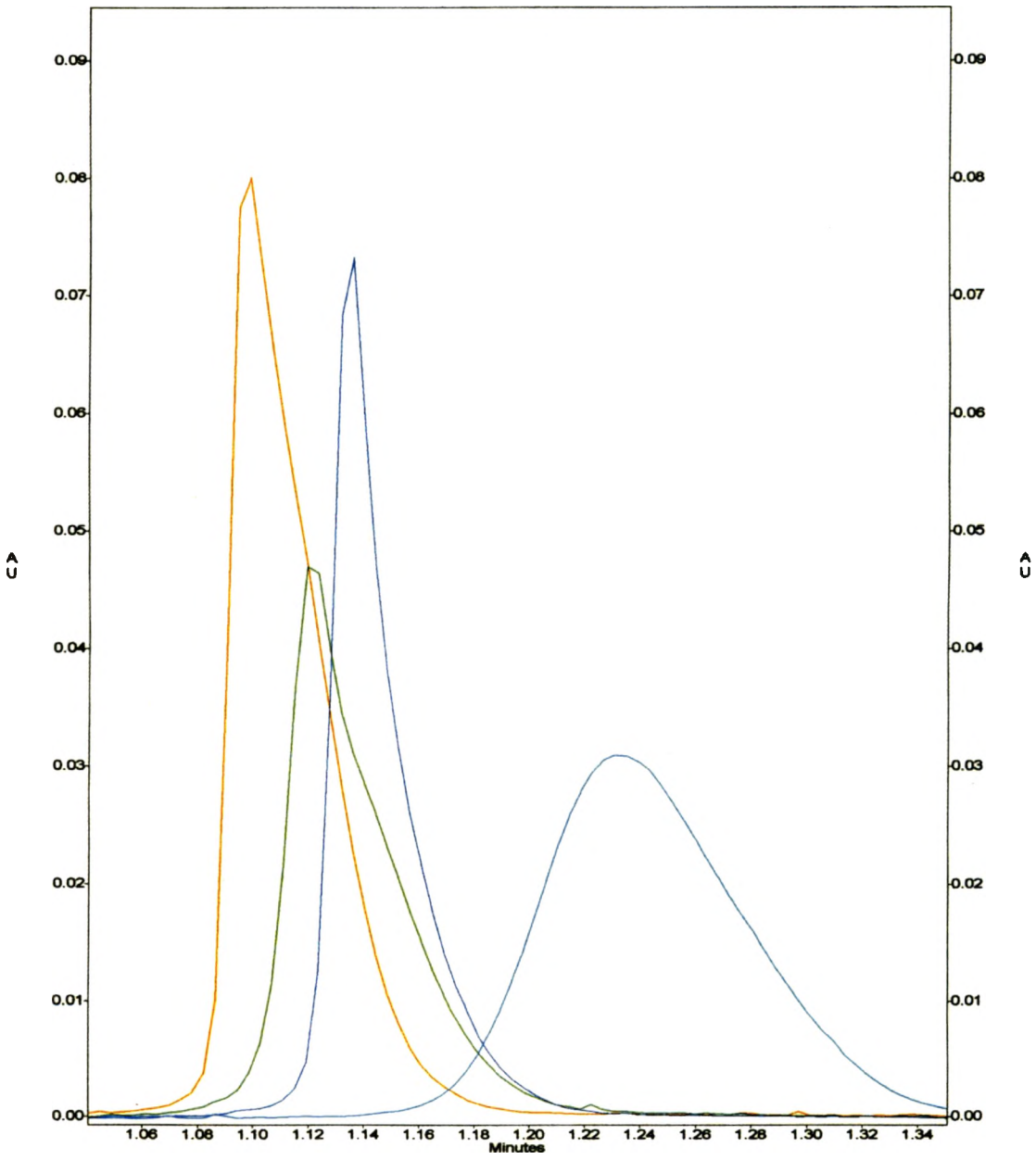

Figure 19: CZE of HSA and the products of the reactions between HSA and the polyhedral borane anions: gold line – HSA, green line – HSA-$B_{20}H_{18}$, dark blue line – HSA-$B_{20}H_{17}OH$, light blue line – HSA-$B_{20}H_{17}SH$

with respect to covalent bond formation or electrostatic interaction cannot be determined from this data.

High Performance Liquid Chromatography. Samples of HSA and the products formed from the reaction of HSA and the polyhedral borane anions were evaluated by reverse phase high performance liquid chromatography (HPLC). HPLC separates the mixture, ideally, into individual components based on the interaction of the species with the hydrophobic column material. Denatured and non-denatured samples were evaluated to ascertain whether any non-covalently bound polyhedral borane anion could be washed from the protein, resulting in a different chromatogram. If the non-denatured samples had a significant amount of polyhedral borane anion associated by electrostatic interactions, and the denaturation succeeded in removing that material from the urea treated samples, then a shift accompanied by a change in shape might be expected in the denatured samples.

The overlapping chromatograms, non-denatured (red line) and denatured (black line), of the HSA and the product of the reaction between HSA and each of the polyhedral borane anions is shown in Figure 20. While there is a small, but noticeable, shift in elution time for the HSA-polyhedral borane complexes in the denatured samples, as compared to the non-denatured samples, the most striking feature in both sets of chromatograms is the consistent difference in the shape of each peak without regard to denaturation.

The HSA control has, as expected, a symmetrical, sharp and narrow peak. Denaturation of the HSA does not significantly alter the chromatogram of the HSA, verifying that the interaction of the protein with the column is not significantly altered

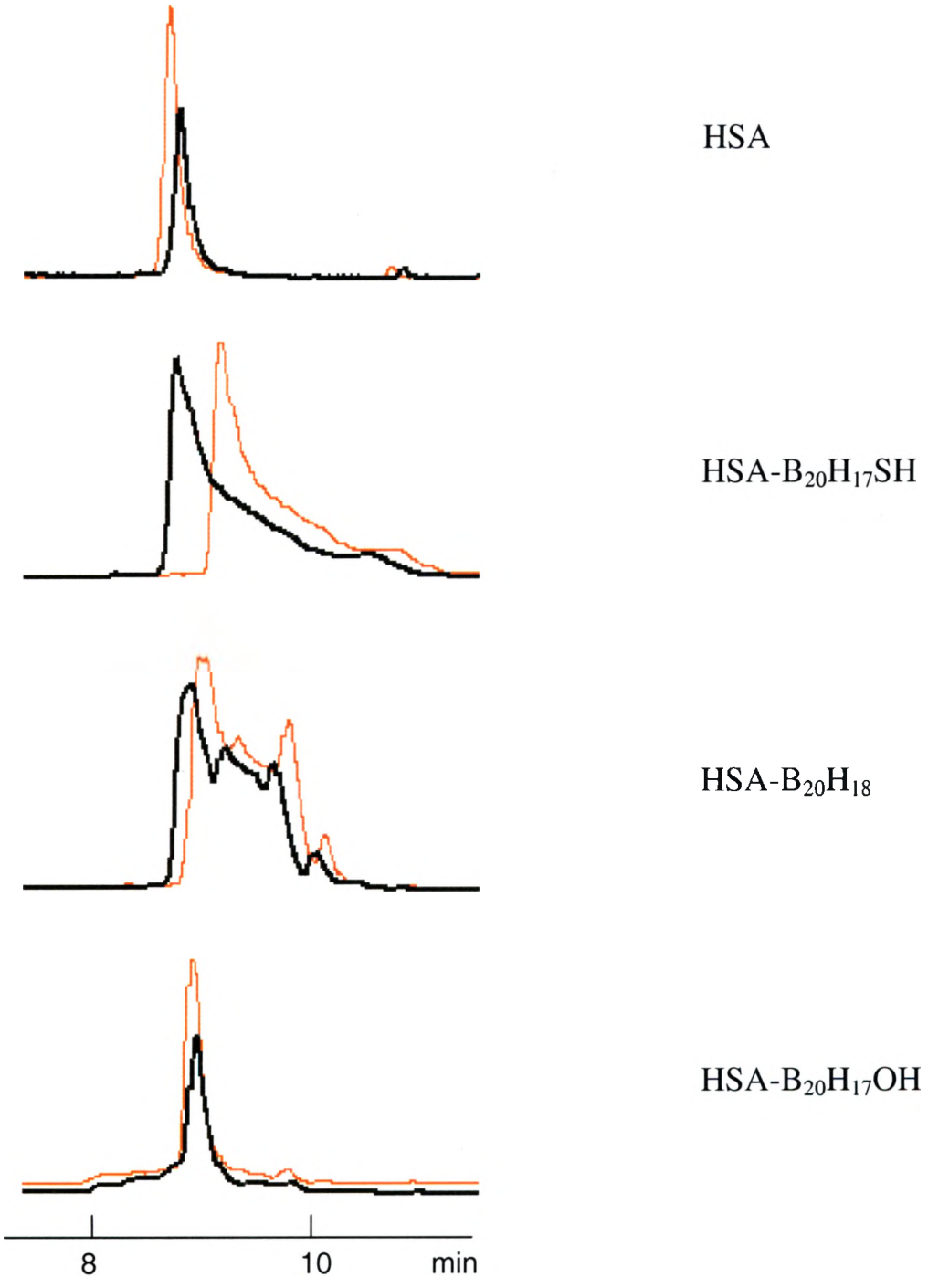

Figure 20: HPLC chromatograms of HSA and the products of the reaction between HSA and the polyhedral borane anions: red lines correspond to the non-denatured samples, black lines correspond to the denatured samples

during the denaturation process. The HPLC chromatogram of the HSA-$B_{20}H_{17}SH$ complex is noticeably broadened, compared to the unreacted HSA, which may indicate a variable number of polyhedral borane anions attached to each HSA molecule and/or the presence of the polyhedral borane anion in different binding sites. The small peak at the far end of the chromatogram may indicate an increased quantity of one type of complex; however, there is no indication as to whether the bonding that is taking place is covalent or electrostatic in nature. The chromatogram of the HSA-$B_{20}H_{18}$ complex produces the most noticeable differences in peak shape. The distinct peaks, though overlapping, may indicate that specific sites on the protein are more likely to react with the polyhedral borane anion. Since the characteristic reactivity of the $[B_{20}H_{18}]^{2-}$ anion is the susceptibility to nucleophilic attack, the distinct peaks in the chromatogram may represent the reaction with specific amino acids that are more likely to act as nucleophiles. The chromatogram of the HSA-$B_{20}H_{17}OH$ complex is very similar to unreacted HSA. The $[B_{20}H_{17}OH]^{4-}$ anion is known to be unreactive in physiological conditions and is unlikely to react with the protein moieties. The HPLC chromatogram supports the known chemistry of the anion.

The complexation of several polyhedral borane anions to HSA should result in a more polar environment and therefore, should exhibit less interaction with the hydrophobic material in the column. As a result, the HSA-polyhedral borane anion complexes should elute faster than the unreacted HSA. Although there is very little difference in the elution time between HSA and the HSA-polyhedral borane anion complexes, the uncomplexed HSA elutes slightly ahead of the bound HSA. The large

negative charge on the polyhedral borane anion cages may be negated by the size of the 66 kD protein.

The shift of the peaks in the chromatograms of the denatured HSA-$B_{20}H_{17}SH$ and HSA-$B_{20}H_{18}$ as compared to the non-denatured species may indicate that some non-covalently bound compound was removed from each of the HSA-polyhedral borane complexes by the denaturation process. The absence of the shift in the HSA-$B_{20}H_{17}OH$ may indicate the absence of non-covalently bound polyhedral borane anion.

The results of the HPLC investigation indicate that there is an interaction between the HSA and both the $[B_{20}H_{18}]^{2-}$ and $[B_{20}H_{17}SH]^{4-}$ anions. The conclusion is supported by both the change in shape of the peaks in the chromatogram as well as the change in elution time. However, the nature of the binding is not clarified.

Trypsin Digests. Samples of the unreacted HSA and the products of the reaction between HSA and the polyhedral borane anions were treated with the enzyme trypsin in order to digest the protein into polypeptide fragments. Trypsin digests or breaks the peptide bond of the protein at the C-terminal side of the amino acids lysine and arginine.[47] The digested samples were evaluated by HPLC.

The chromatograms of the digested protein and protein complexes were compared to each other for the purpose of identifying shifts or changes in peak shape between different fractions, indicating a possible binding location on the protein of one or more of the polyhedral borane anions. Samples that were treated with dithiothreitol and samples that were not treated with dithiothreitol were compared to each other. The dithiothreitol, which breaks disulfide bonds, would separate distinct polypeptide fragments into smaller units. Small changes in molecular weight would be more easily identified with the

smaller polypeptide fragments. The negative consequence of treating the sample with DTT is that one of the primary binding modes of interest is the formation of a disulfide bond between the free sulfhydryl on HSA at cysteine 34 and the sulfhydryl on the $[B_{20}H_{17}SH]^{4-}$ anion. The reduction of a potential bond between these two entities when compared to the sample that is not reduced may provide evidence of disulfide formation. The reduction of an internal disulfide bond in the protein may complicate this identification.

When the reduced samples and the non-reduced samples are compared (Figures 21 and 22), there are noticeable differences in several locations. As a portion of the future research associated with the research project, the fragments of the protein and protein complexes will be identified and characterized by MALDI-MS.

Glutathione Reaction. The $[B_{20}H_{17}SH]^{4-}$ anion was allowed to react with glutathione, both in the oxidized and in the reduced form. The goal of the reaction was to identify the formation of a disulfide bond. The products of the reactions were evaluated by HPLC (Figure 23). Although there is an apparent difference in the chromatograms, the interpretation of the results is complicated by the fact that the unreacted polyhedral borane anion was not washed from the reaction mixture. The experiment will be repeated with the correction and the results reevaluated.

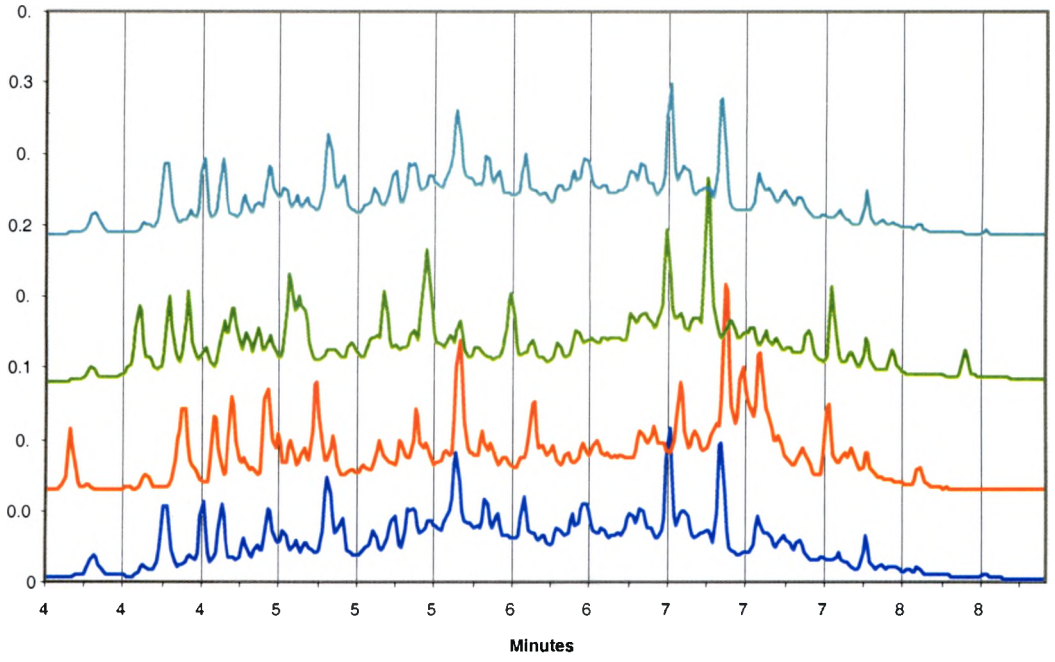

Figure 21: HPLC chromatograms of the **non-reduced** trypsin digest of HSA and the products of the reaction between HSA and the polyhedral borane anions: dark blue — HSA, red — HSA-$B_{20}H_{17}SH$, green line — HSA-$B_{20}H_{18}$, light blue — HSA-$B_{20}H_{17}OH$

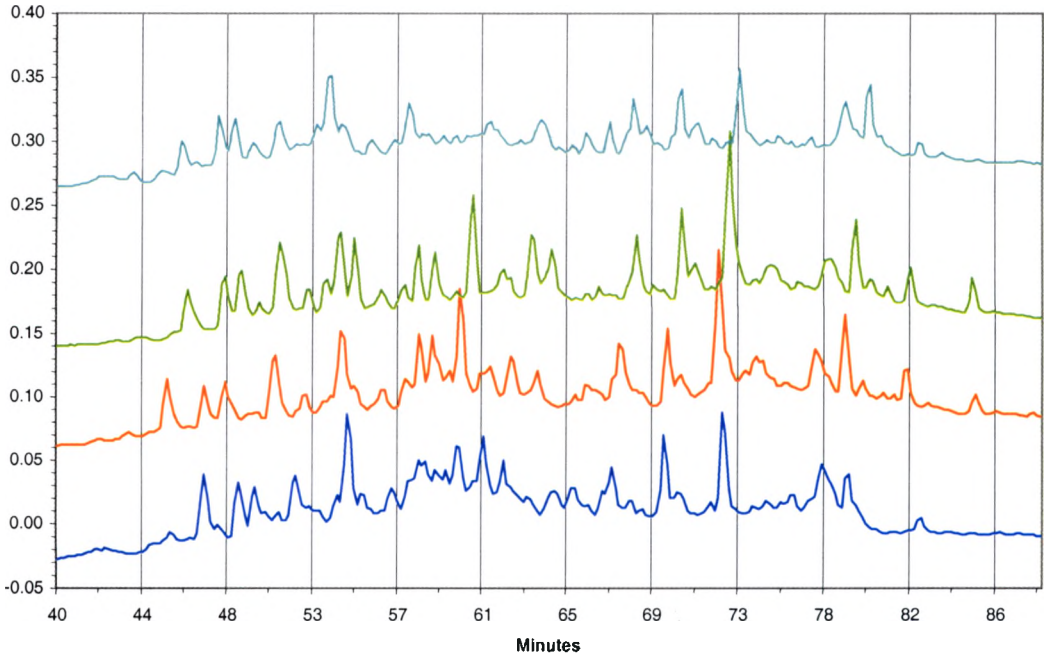

Figure 22: HPLC chromatograms of the **reduced** trypsin digest of HSA and the products of the reaction between HSA and the polyhedral borane anions: dark blue — HSA, red — HSA-$B_{20}H_{17}SH$, green line — HSA-$B_{20}H_{18}$, light blue — HSA-$B_{20}H_{17}OH$

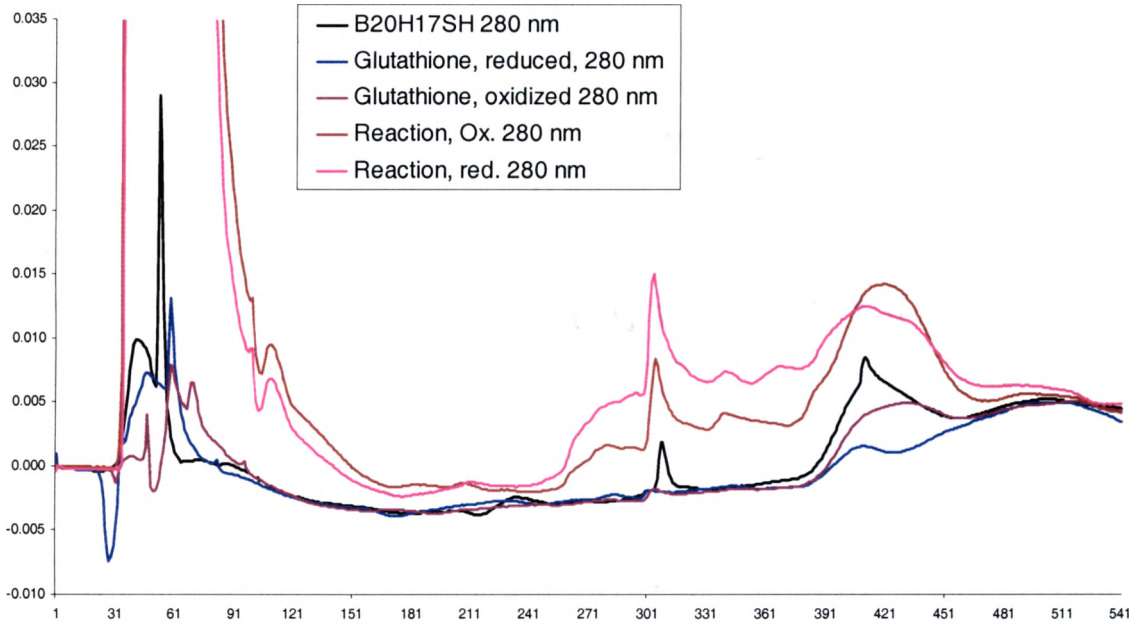

Figure 23: HPLC chromatogram of the glutathione reaction with the $[B_{20}H_{17}SH]^{4-}$ anion

CHAPTER 5

CONCLUSIONS

The goal of this research project was to determine the nature of the long-term retention demonstrated by specific polyhedral borane anions in murine biodistribution studies. Although researchers have proposed that the retention of the polyhedral borane anions was a result of covalent bond formation with intracellular protein moieties, there have been no investigations reported that demonstrate the formation of a covalent bond between a polyhedral borane anion and any protein. Therefore, polyhedral borane anions were selected based on their different retention properties in biodistribution studies. The polyhedral borane anion $[B_{20}H_{17}SH]^{4-}$ was selected based on the demonstrated accretion of boron in the tumor while $[B_{20}H_{18}]^{2-}$ and $[B_{20}H_{17}OH]^{4-}$ were chosen for their moderate and small tumor retention, respectively. The polyhedral borane anions were allowed to react with bovine serum albumin and human serum albumin and the results of the reactions were evaluated by a number of analytical techniques, including SDS-PAGE, MALDI-MS, HPLC, and CZE.

The products of the reaction between BSA and each of the polyhedral borane anions were evaluated initially using SDS-PAGE analysis. The anticipated increase in mass, as a result of the interaction of the protein with the polyhedral borane anions, was not observed. Based on the observed increase in mass in the MALDI-MS spectra, it is believed that the SDS-PAGE resolution is not sufficient to observe the relatively small increases. In addition, the inclusion of DTT in the samples should reduce any disulfide bonds that might have formed between $[B_{20}H_{17}SH]^{4-}$ and the thiol substituent on cysteine

34 of the albumins. Therefore, future investigations using SDS-PAGE as the analytical tool were abandoned.

The increase in mass that was observed in the MALDI-MS analysis of the product of the reaction of BSA or HSA and the polyhedral borane anion, $[B_{20}H_{17}OH]^{4-}$, was within the predicted error for the experiment. The relatively small increase exhibited in either case indicated a minimal interaction. The HPLC and CZE data for the product of the reaction of HSA and the $[B_{20}H_{17}OH]^{4-}$ anion was minimally distinguishable from that of the HSA control when both elution times and peak shape are compared. Therefore, the results of the analysis indicate that the polyhedral borane anion, $[B_{20}H_{17}OH]^{4-}$, is essentially unreactive.

MALDI-MS analysis of the product of the reaction of HSA and the polyhedral borane anion, $[B_{20}H_{18}]^{2-}$, reveals a relatively large shift in molecular weight which would indicate a strong interaction had taken place. The broadening of the peak is consistent with different numbers of polyhedral borane anions attached to the HSA molecules. The HPLC chromatograms reveal substantial peak broadening and a consistent change in shape providing an indication of binding at specific locations. The results of the analysis may indicate that the polyhedral borane anion $[B_{20}H_{18}]^{2-}$ is reacting with nucleophilic protein moieties, but a strong electrostatic interaction between the protein and the negative charge cannot be dismissed. The reactivity of the polyhedral borane anion $[B_{20}H_{18}]^{2-}$ is supported by murine biodistribution studies.

The $[B_{20}H_{17}SH]^{4-}$ anion is the only ion of the three studied that demonstrated accretion of boron within the tumor mass in murine biodistribution studies. MALDI-MS analysis demonstrates an increase in molecular weight that is similar to that of the

$[B_{20}H_{18}]^{2-}$ anion. The broadness of the peak would again suggest that more than one binding site has been occupied by the $[B_{20}H_{17}SH]^{4-}$ anion, either electrostatically or covalently. The polyhedral borane anion contains a sulfhydryl group which is available for disulfide formation and the experiments with DTNB indicate that at least some disulfide formation is taking place between the protein and the polyhedral borane anion. The HPLC chromatogram for the $[B_{20}H_{17}SH]^{4-}$ anion is broad with a small peak near the tail of the parent signal, possibly indicating a specifically bound product.

The trypsin digests for all of the polyhedral borane anions that had undergone the reaction protocol with HSA produced HPLC chromatograms revealing peak shifts and shape changes that could be binding sites. The shifts observed in the chromatograms of the HPLC analysis of the trypsin digest forms the basis of future research and the possible identification of the specific binding sites.

In summary, the $[B_{20}H_{17}OH]^{4-}$ anion, which is known to be unreactive in physiological conditions, did not demonstrate any significant interaction with the albumins. The more reactive $[B_{20}H_{18}]^{2-}$ and $[B_{20}H_{17}SH]^{4-}$ anions did demonstrate a strong interaction with the proteins. Although there is no unequivocal evidence that the binding of the polyhedral borane anions to the albumins is covalent, the lack of interaction by the $[B_{20}H_{17}OH]^{4-}$, a highly charged polyhedral borane anion, may indicate that something other than electrostatic interaction is present.

CHAPTER 6

PROSPECTS FOR FUTURE RESEARCH

The immediate task that lies ahead is to characterize the nature of the interaction discovered between the polyhedral borane anions and the albumins investigated in this study. There are a number of investigative procedures that might be employed to affect the desired outcome. The fractions collected from the trypsin digest and subsequent HPLC analysis of the reduced and non-reduced HSA will be analyzed by MALDI-MS in an effort to locate areas of increased mass on single polypeptide chains. Once the polypeptide fragment containing the polyhedral borane anion has been identified, the fragment can be sequenced by data base search or known sequencing techniques, such as Edman Degradation.

A thorough investigation of the potential reactions with individual amino acids or small metabolites, such as glutathione which has a free sulfhydryl group in its reduced form, would be beneficial. The products of the reactions could be analyzed using the same analytical techniques. Once reactive sites have been identified, one could possibly synthesize an appropriately reactive polypeptide and attempt to grow a crystal. X-ray diffraction could elucidate the crystal structure, permitting insight into the nature of the bonding and also the potential binding properties of future compounds.

Knowledge of the precise nature of the interaction of the polyhedral borane anions and biomolecules would enhance the ability of boron chemists to design boron compounds that more effectively localize in tumor masses. The selective accretion of

boron in tumor masses enables the potentially live saving, or quality of life enhancing, procedure of boron neutron capture therapy for thousands of people.

REFERENCES

1. Soloway, A. H., Tjarks, W., Barnum, B.A., Rong, R-G., Barth, R. F., Codogni, I. M. & Wilson, J. G. (1998) *Chem. Rev.* **98**, 1515-1562.
2. Friedlander, G., Kennedy, J. W., Macias, E. S., Miller, J. M. *Nuclear and Radiochemistry*, 3rd Ed., John Wiley: New York, 1981.
3. Hawthorne, M.F. (1993) *Angew. Chemie Int. Ed. Eng.* **32(7)**, 950-984.
4. Locher, G.L. (1936) *Am. J. Roentgenol. Radium Ther.* **36**, 1-13.
5. Fairchild, R. G. & Bond, V. P. (1985) *J. Radiat. Oncol. Biol. Phys.* **11**, 831-840.
6. Soloway, A. H., Barth, R. F., Alam, F. In: *Boron Neutron Capture Therapy for Tumors*, Hatanaka, H. (Ed) Nishiura, Niigata, 1986, pp. 47-58.
7. Abe, M., Amano, K., Kitamura, K., Ohta, M., Tateishi, J., Hatanaka, H. (1988) *Neurosurgery* **22**, 123-130.
8. Clendenon, N.R., Barth, R. F., Gordon, W. H., Alam, R., Soloway, A. H., Staubus, A.E., Boesel, C. P., Yates, A. J., Noeschverger, N. C., Gahbauer, R., Fairchild, R. G., Slatkin, D. N., Kalef-Ezra, J. (1990) *Neurosurgery* **26**, 47-55.
9. Radel, P. A. & Kahl, S. B. (1996) *J. Org. Chem.* **61**, 4582.
10. Srivastava, R. R. & Kabalka, G. W. (1997) *J. Org. Chem.* **62**, 8730-8734.
11. Srivastava, R. R., Singhaus, R. R. & Kabalka, G. W. (1997) *J. Org. Chem.* **62**, 4476-4478.
12. Schinazi, R. F. & Prusoff, W. H. (1978) *Tetrahedron Lett.* **50**, 4981.
13. Yamamoto, Y., Seko, T., Nemoto, H. (1989) *J. Org. Chem.* **54**, 4735.
14. Sood, A., Shaw, B. R. & Spielvogel, B. F. (1989) *J. Am. Chem. Soc.* **111**, 9234.
15. Li, H., Hardin, C. & Shaw, B. R. (1996) *J. Am. Chem. Soc.* **118**, 6606.
16. Hawthorne, M. F. (1991) *Pure Appl. Chem.* **63**, 327-334.
17. Hill, J. S., Kahl, S. B., Kaye, A. H., Stylli, S. S., Koo, M.-S., Gonzales, M. F., Vardaxis, N. J. & Johnson, C. I. (1992) *Proc. Natl. Acad. Sci. USA* **89**, 1785-1789.
18. Yamamoto, Y. (1997) *Special Publication of the Royal Society of Chemistry* **201** (Advances in Boron Chemistry), 281-288.
19. Laster, B. H., Kahl, S. B., Popenoe, E. A., Pate, D. A. & Fairchild, R. G. (1991) *Cancer Res.* **51**, 4588.
20. Shelly, K., Feakes, D. A., Hawthorne, M. F., Schmidt, P. G., Krisch, T. A. & Bauer, W. F. (1992) *Proc. Natl. Acad. Sci. USA* **89**, 9039-9043.
21. Feakes, D. A., Shelly, K., Knobler, C. B. & Hawthorne, M. F. (1994) *Proc. Natl. Acad. Sci USA* **91**, 3029-3033.
22. Feakes, D.A., Shelly, K., & Hawthorne, M. F. (1995) *Proc. Natl. Acad. Sci USA* **92**, 1367-1370.
23. Feakes, D. A., Waller, R. C., Hathaway, D. K. & Morton, V. S. (1999) *Proc. Natl. Acad. Sci USA* **96**, 6406-6410.
24. Juliano, R. L. & Stanys, D. (1978) *Biochem Pharmacol.* **27**, 21-27.
25. Forssen, E. A. & Tokes, Z. A. (1983) *Cancer Res.* **43**, 546-550.
26. Rahman, A., Fumagalli, A., Barbieri, B., Schein, P. & Casazza, A. M. (1986) *Cancer Chemother. Pharmacol.* **16**, 22-27.

27. Straubinger, R. M., Hong, K., Friend, D. S. & Papahadjopoulos (1983) *Cell* **32**, 1069-1079.
28. Coderre, J. A., Kalef-Ezra, J. A., Fairchild, R. D., Micca, P. L., Reinstein, L. E. & Glass, J. D. (1988) *Cancer Res.* **48**, 6313-6316.
29. Clendonen, N. R., Barth, R. F., Gordon, W. A., Goodman, J. H., Alam, F., Staubus, A. E., Boesel, C. P., Yates, A. J., Moeschberger, M. L., Fairchild, R. G. & Kalef-Ezra, J. A. (1990) *Neurosurgery* **26**, 47-55.
30. Gabel, D., Holstein, H., Larsson, B., Gille, L., Ericson, G., Sacker, D., Som, P. & Fairchild, R. G. (1987) *Cancer Res.* **47**, 5451-5454.
31. Slatkin, D., Micca, P., Forman, A., Gabel, D., Wielopolski, L. & Fairchild, R. G. (1986) *Biochem. Pharmacol.* **35**, 1771-1776.
32. Soloway, A. H., Hatanaka, H. & Davis, M. A. (1967) *J. Medicinal Chem.* **10**, 714-717.
33. Sweet, W. H., Soloway, A. H. & Wright, R. L. (1962) *J. Pharmacol. Exp. Ther.* **137**, 263-266.
34. Hawthorne, M. F., Pilling, R. L., Stokely, P. F. & Garrett, P. M. (1963) *J. Am. Chem. Soc.* **85**, 3704.
35. Hawthorne, M. F., Pilling, R. L. & Garrett, P. M. (1965) *J. Am. Chem. Soc.* **87**, 4740-4746.
36. Hawthorne, M. F. & Pilling, R. L. (1967) *Inorg. Synth.* **9**, 16-19.
37. Chamberland, B. L. & Muetterties, E. L. (1964) *Inorg. Chem.* **3**, 1450-1456.
38. Daly, W. H. & Lee, C. S. (1973) *Polymer Preprints* **14**, 1238-1243.
39. Sergupta, S., Chen, H., Togawa, T., DiBello, P. M., Majors, A. K., Budy, B., Ketterer, M. E. & Jacobson, D. W. (2001) *J. Biol. Chem.* **276**, 30111-30117.
40. Peters, T., Jr. (1985) *Adv. Protein Chem.* **37**, 161-245.
41. Sigma Product Information Sheet, CAS Number 9048-46-8, Product Catalog Number A-7638.
42. Neans, G. E. & Feeney, R. E. *Chemical Modifications of Proteins* (1971) Holden-Day, Inc., pg. 155.
43. Sigma Product Information Sheet, CAS Number 70024-90-7, Product Catalog Number A-8763.
44. Mahdy, M. A., El-Ghamry, H. A. & Ismail, A. (1999) *Zagazig J. Pharm Sci.* **8(1)**, 68-75.
45. Hong, L., Bian, H-D., Tu, C-Q. & Shen, P-W. (2001) *Gaodeng Xuexiao Huaxue Xuebao* **22(1)**, 21-25.
46. Moriyama, Y. & Takeda, K. (1999) *Langmuir* **15**, 2003-2008.
47. Tropp, B. E. *Biochemistry: Concepts and Applications* (1997) Brooks/Cole Publishing Company, pg. 127.

VITAE

Jeff McVey was born in Corpus Christi, Texas, on May 22, 1950, the son of William J. McVey and Dollie Ann McVey. After completing high school at Frederick Military Academy (Portsmouth, Virginia) in 1968, he entered the University of Mississippi in Oxford, Mississippi. Jeff spent four years in the US Air Force as a member of the elite Pararescue Force from 1973 to 1977. He graduated with a business degree in 1980 from the University of Texas at Dallas. In 1996, Jeff enrolled at Southwest Texas State University and graduated with a B.S. in Chemistry in 2000.

Permanent Address: PO Box 1086
Lockhart, TX 78644

This thesis was typed by Jeff McVey.